View metadata, citation and similar papers at core.ac.uk

brought to you by CORE

provided by Edge Hill University Research Information Repository

NeuroImage 202 (2019) 116133

Contents lists available at ScienceDirect

NeuroImage

journal homepage: www.elsevier.com/locate/neuroimage

Frontal cortex differentiates between free and imposed target selection in multiple-target search

Eduard Ort [a,b,*], Johannes J. Fahrenfort [a,b,c], Reshanne Reeder [d,e], Stefan Pollmann [d,e], Christian N.L. Olivers [a,b]

[a] Department of Experimental and Applied Psychology, Vrije Universiteit Amsterdam, van der Boechorststraat 7, 1081 BT, Amsterdam, the Netherlands
[b] Institute for Brain and Behavior Amsterdam, Vrije Universiteit Amsterdam, van der Boechorststraat 7, 1081 BT, Amsterdam, the Netherlands
[c] Department of Brain and Cognition, University of Amsterdam, Nieuwe Achtergracht 129 B, 1018WS, Amsterdam, the Netherlands
[d] Center for Behavioral Brain Sciences, Otto-von-Guericke University Magdeburg, Universitätsplatz 2, 39106, Magdeburg, Germany
[e] Department of Experimental Psychology, Otto-von-Guericke University Magdeburg, Universitätsplatz 2, 39106, Magdeburg, Germany

ARTICLE INFO

Keywords:
Visual attention
Proactive cognitive control
Reactive cognitive control
Visual search
Eye movements
Functional magnetic resonance imaging

ABSTRACT

Cognitive control can involve proactive (preparatory) and reactive (corrective) mechanisms. Using a gaze-contingent eye tracking paradigm combined with fMRI, we investigated the involvement of these different modes of control and their underlying neural networks, when switching between different targets in multiple-target search. Participants simultaneously searched for two possible targets presented among distractors, and selected one of them. In one condition, only one of the targets was available in each display, so that the choice was imposed, and reactive control would be required. In the other condition, both targets were present, giving observers free choice over target selection, and allowing for proactive control. Switch costs emerged only when targets were imposed and not when target selection was free. We found differential levels of activity in the frontoparietal control network depending on whether target switches were free or imposed. Furthermore, we observed core regions of the default mode network to be active during target repetitions, indicating reduced control on these trials. Free and imposed switches jointly activated parietal and posterior frontal cortices, while free switches additionally activated anterior frontal cortices. These findings highlight unique contributions of proactive and reactive control during visual search.

1. Introduction

During search for a visual object, a mental representation of the target object is maintained in visual working memory to guide attention toward potentially task-relevant regions (Desimone and Duncan, 1995; Olivers and Eimer, 2011). In everyday situations, individuals may oftentimes try to find multiple objects at the same time, which would require the maintenance of more than one target representation. It has been shown that such multiple-target search can be challenging, often resulting in reduced search performance (Barrett and Zobay, 2014; Dombrowe et al., 2011; Found and Müller, 1996; Juola et al., 2004; Liu and Jigo, 2017; Maljkovic and Nakayama, 1994; Menneer et al., 2007), raising the question as to how these multiple target representations are established for, and updated during, search – in other words, how these representations are controlled.

Recent work from one of our labs suggests that when observers look for more than one target, they may dynamically prioritize one of multiple potential target representations to guide search at any given moment (Ort et al., 2017, 2018). Specifically, we found that performance in multiple-target search depends on whether or not observers are given the opportunity to freely choose the target to select. In a gaze-contingent search paradigm, observers were instructed to always find one of two potential target colors. Importantly, they could either freely select the target to look for on a particular trial, as both targets would always be available in each search display, or the choice was imposed upon them, as only one of the two targets would be present on each trial. Eye movement latencies showed that, relative to target repeats, target switches were more costly when imposed than when made under free choice conditions. In further support of this, van Driel et al. (2019) recently conducted electroencephalography (EEG) measurements during free and imposed

* Corresponding author. Vrije Universiteit Amsterdam, van der Boechorststraat 7, 1081 BT, Amsterdam, the Netherlands.
E-mail addresses: eduardxort@gmail.com (E. Ort), fahrenfort.work@gmail.com (J.J. Fahrenfort), reshanne.reeder@ovgu.de (R. Reeder), stefan.pollmann@ovgu.de (S. Pollmann), c.n.l.olivers@vu.nl (C.N.L. Olivers).

https://doi.org/10.1016/j.neuroimage.2019.116133
Received 8 March 2019; Received in revised form 22 July 2019; Accepted 24 August 2019
Available online 28 August 2019
1053-8119/© 2019 The Authors. Published by Elsevier Inc. This is an open access article under the CC BY license (http://creativecommons.org/licenses/by/4.0/).

choice, and found that free switching between targets is associated with *pre-trial* power suppression in the beta band over midfrontal electrodes – a signal that has been linked to choice behavior (Donner et al., 2009; Spitzer and Haegens, 2017). In contrast, forced target switches elicited *post-trial* power enhancement in the delta/theta band – a signal that has been associated with conflict detection (Cavanagh and Frank, 2014; Cohen, 2014; Duprez et al., 2018). We interpret these eye movement and EEG findings within an influential framework proposed by Braver (2012), which assumes a division of cognitive control into two modes: *proactive* and *reactive* control. Proactive control is invoked and maintained in anticipation of a task, whereas reactive control is triggered whenever a conflict or unexpected event occurs. In multiple-target search, the availability of all targets in a display allows for proactive control, as observers can freely prepare for either target (cf. Arrington and Logan, 2004, 2005; Meiran, 1996). In contrast, imposing a target (i.e. by only presenting only one of the two targets in the search display) would invoke reactive control, which is reflected in a costly switching of attentional priority to the only available target. In the present study we sought to uncover the brain areas underlying free and imposed multiple-target search.

1.1. Brain areas involved in different modes of control

Cognitive control has been extensively investigated in the context of the implementation of, and switching between, different task sets (Meiran, 2010; E. K. Miller and Cohen, 2001). Task switches have been associated with brain regions that are considered part of a general cognitive control network that is distributed mainly over frontoparietal regions of the brain (Cole and Schneider, 2007; Dosenbach et al., 2006; Dosenbach et al., 2008; Duncan, 2010; Dove et al., 2000; Fedorenko et al., 2013; Kim et al., 2012; Liston et al., 2006; Power and Petersen, 2013, A. B. Smith et al., 2004). However, it is unknown whether similar brain areas are also involved in switching representations within one and the same task, which is the case when observers hold multiple target representations for the same visual search task, and how this would differ for circumstances that enable different modes of control.

The distinction between proactive and reactive control has mostly been studied in the context of interference control across various domains, such as interference between competing working memory representations (Burgess and Braver, 2010; Marklund and Persson, 2012), between competing visual stimuli (De Pisapia and Braver, 2006; Jiang et al., 2015), or between competing stimulus-response mappings (Braver et al., 2003; Jiang et al., 2018; Ryman et al., 2018; Sohn et al., 2000). The mode of control is commonly induced by manipulating the likelihood (or predictability) of upcoming interference, following the assumption that whenever individuals anticipate interference, they will strengthen proactive control. Some studies suggest that proactive and reactive control are governed by different brain areas, but the findings are somewhat inconsistent, which may be related to the different paradigms used, and to an emphasis on differences in the temporal dynamics (with proactive assumed to occur prior to task onset, while reactive follows conflicting events). Based on their reviews of the literature, Braver (2012) as well as Irlbacher et al. (2014) have suggested that both modes of control are governed by a similar set of brain areas, but might be activated with different dynamics, as proactive control can be instantiated in advance. These areas include the lateral prefrontal cortex and posterior parietal cortex, with relatively minor differences between them, whereas reactive control may additionally recruit midfrontal regions when there is conflict detection involved. Similar brain areas may therefore be involved during control over target selection in multiple-target search.

Target selection in multiple-target search is associated with shifts in feature-based attention between target-defining features. Such shifts of feature-based attention have previously been linked to activity primarily in posterior parietal (i.e. superior parietal lobule) and posterior, lateral frontal regions (i.e. inferior frontal junction and dorsal premotor cortex; Greenberg et al., 2010; Liu et al., 2003; Pollmann et al., 2006; Pollmann et al., 2000; Slagter et al., 2006, 2007; Wager et al., 2004). However, in most of these studies, a feature shift was also associated with a change in response (Greenberg et al., 2010; Liu et al., 2003; Pollmann et al., 2006; Slagter et al., 2006, 2007). Moreover, these studies did not directly compare different modes of control over such shifts. They measured activity in response to either cue- or task-induced changes of the task-relevant feature, but did not juxtapose self-generated (free) to stimulus-induced (imposed) changes.

In one recent study, Gmeindl et al. (2016) did compare cue-induced to self-generated (i.e. freely chosen) shifts of spatial attention. They found similar posterior parietal activity during both types of shifts, while self-generated shifts additionally activated the medial frontal cortex and lateral frontopolar cortex. These medial frontal and frontopolar regions have also previously been shown to be related to voluntary versus imposed action selection (Demanet et al., 2013; Forstmann et al., 2006; Orr and Banich, 2013; Passingham et al., 2010; Soon et al., 2008; Taylor et al., 2008; Wisniewski et al., 2016; Wisniewski et al., 2015; J. Zhang et al., 2013), and have been argued to be involved in the evaluation of alternative goals in the context of exploratory behavior (Mansouri et al., 2017; Pollmann, 2016). The same areas may therefore be involved when observers choose to change target in visual search, but this is currently unknown.

1.2. The present study

We sought to investigate differences in the locus or level of activated brain regions when proactive and reactive control mechanisms operate in a context of multiple-target search. Specifically, we set out to test whether differences between free and imposed switches between targets during visual search for multiple objects are accompanied by differences in brain activity that might be linked to proactive and reactive control processes. To that end, we adopted a fast-paced, gaze-contingent eye tracking paradigm (Ort et al., 2017; illustrated in Fig. 1A) in combination with event-related fMRI. Participants were always instructed to look for two color-defined targets and to make an eye movement towards one of them on every trial. In one block type, both potential targets were present in a search display and participants were free to select either of them. In the other type of block, only one target was present and the choice was imposed. We instructed participants to either make (when choice was free) or expect (when choice was imposed) target switches. We reasoned that free target switches would be associated with proactive, preparatory control mechanisms, while imposed switches would result in reactive, compensatory control mechanisms. Differential neural activity for each switch type would constitute evidence for proactive and reactive control having unique contributions to target selection during multiple-target search. Based on the literature on both task and attention shifts, we expected to find switch-related activity in the posterior parietal and posterior frontal cortex for both switch types. In addition, we were interested to explore potential differences in the control network for free and imposed target switches. In line with the literature on self-generated versus externally-cued choice, we expected activity in the lateral frontopolar cortex as well as the medial frontal cortex to be selectively active during free switches.

2. Methods

2.1. Data and code availability

Data and code was made publicly available on *osf. io* (https://osf.io/a8vxn). Unthresholded statistical maps were uploaded to *neurovault. org* (https://neurovault.org/collections/5550/).

2.2. Participants

A sample of 22 participants (age: 21–35 years, M = 27.3; 10 females, 12 males) was recruited from the subject pool of the Leibniz Institute of

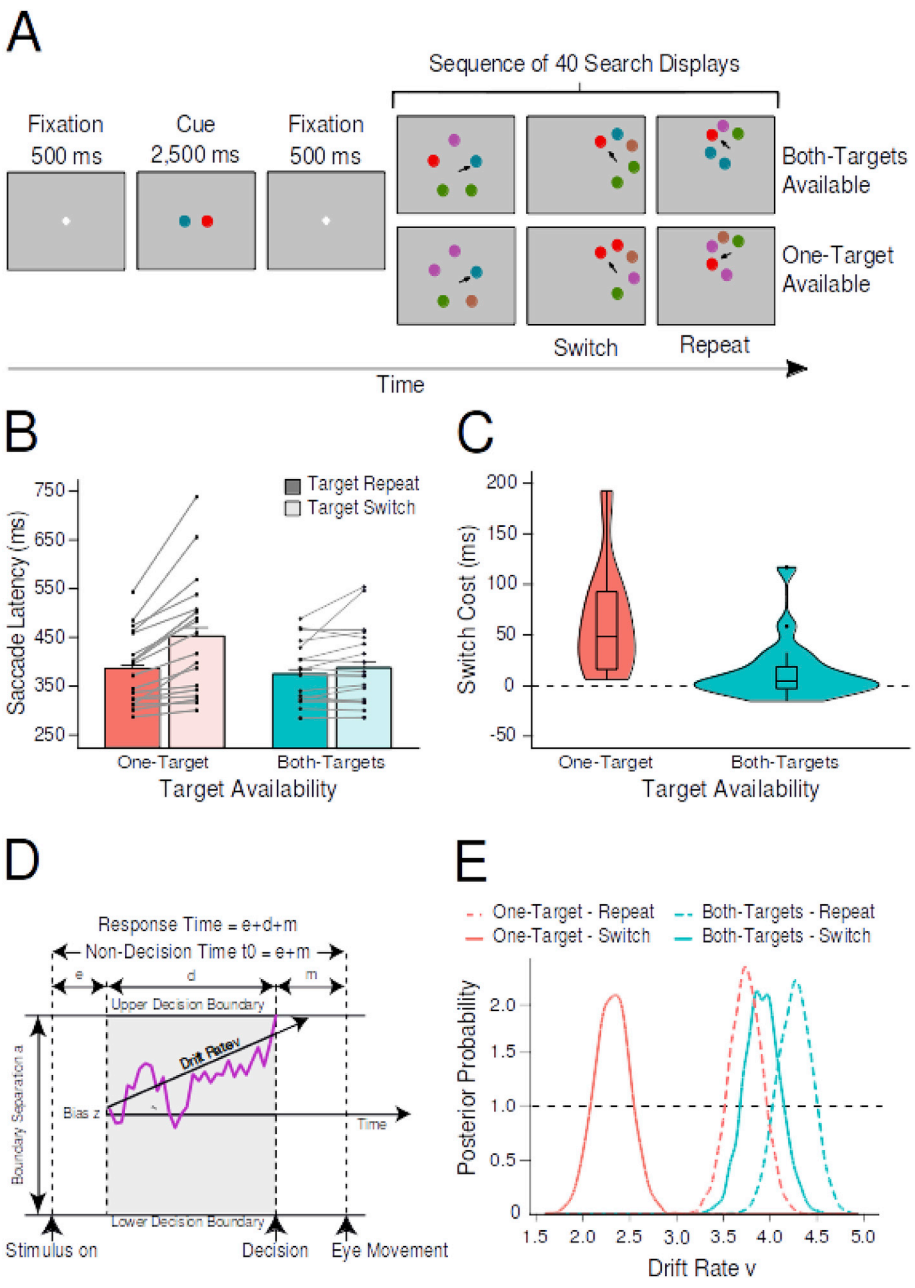

Fig. 1. Illustration of the study design and behavioral results. (A) Each block began with a cue indicating the two target colors for the subsequent sequence of 40 search displays. Depending on the target availability condition, each search display contained either one of the two target colors or both of them. In case of only one target color being available, there could still be two targets carrying that color, to equate for the mere number of targets present (see section 2.3). Participants were required to fixate one of the targets (indicated here by an arrow, which was not present in the display); this triggered the next display, which appeared on an imaginary annulus surrounding the location of the previously fixated target. (B) The bar plots represent the mean saccade latencies on switch trials and repeat trials for each level of target availability (one target vs. both targets). The gray lines represent the mean saccade latencies for each observer individually. Error bars represent the upper limit of the within-subjects 95% confidence intervals (Morey, 2008). (C) The violin plots depict the distribution of switch costs, which were computed by subtracting repeat saccade latencies from switch saccade latencies, separately for the target availability conditions. The horizontal lines in the box plots represent the first, second (median), and third quartiles. The vertical lines represent the distance between minimum (lower quartile - 1.5 * interquartile range) and maximum (upper quartile + 1.5 * interquartile range). Single dots indicate individual outliers. (D) Schematic and simplified equation of a drift diffusion model (adapted from Kloosterman et al., 2019). *e* denotes encoding time, *d* denotes decision time, and *m* denotes motor execution. (E) HDDM results indicating the posterior probability distributions for drift rates, separately for all experimental conditions.

Neurobiology in Magdeburg. Three individuals were excluded due to insufficient eye tracking accuracy, reducing the final sample to 19 participants. All participants gave written consent according to the Declaration of Helsinki and were reimbursed with 30 Euros. They reported normal or corrected-to-normal visual acuity and color vision and were naive to the purpose of the experiment. The study was approved by the research ethics board of Otto-von-Guericke University Magdeburg.

2.3. Stimuli, procedure, and design

The stimulus set consisted of five colored disks with a radius of 0.6° visual angle (dva). These colors were blue (RGB-values: 0, 130, 150), red (240, 0, 0), green (70, 135, 0), brown (175, 100, 75), and purple (180, 80, 170). All stimulus colors were isoluminant ($M = 21$ cd/m^2) and presented on a uniform gray background (197, 197, 197). A search display was composed of five disks placed on an imaginary annulus around fixation with a radius randomly drawn from values between 3.6 and 4.4 dva around the starting point. Any two adjacent disks had an angular distance of at least 45°.

A block was initiated once participants steadily fixated a central white dot. First, a white fixation cross was presented in the center of the screen for 500 m s, followed by the cue display for 2500 m s and another fixation cross for 500 m s (Fig. 1A). In the cue display, two colored disks were presented 1.0 dva to the left and right of fixation to mark these colors task-relevant for the upcoming sequence of 40 search displays. In each search display, participants were required to select a target-colored disk among a set of five disks by making a saccade toward it. After target fixation, the search display disappeared and the fixated target was replaced by a black ring to provide participants with a fixation point during the intertrial interval (uniformly jittered between 950 and 1050 m s). Because the coordinates of the previously fixated target served as the starting point for the next display, the search displays moved across the screen throughout a block. To make sure that search displays would fall within the margins of the screen, stimuli were moved closer to each other on that part of the annulus that was closest to the center of the screen, whenever a search display approached an edge of the screen.

Importantly, the relative positions of the targets in the search display remained unpredictable. Saccades had to land within a radius of 0.9 dva to the center of a target to trigger the next search display. If participants fixated one of the distractors, they received auditory error feedback and were required to make a corrective eye movement toward a target. The search was aborted if no target was fixated within 3000 m s, and a new search display appeared, centered at the same location.

There were two main factors in this experiment: *target availability* (whether only one or both targets were present in the search display), and *transition type* (whether target selection switched or repeated from one trial to the next). The target availability factor was controlled at the block level by presenting either only one, or both of the targets in the display. In the *both-targets condition*, both cued targets appeared in the search display. In the *one-target condition*, only one of the targets was present. The transition type factor (*target repeat* vs. *target switch*) was determined by the observer (both-targets blocks) or by a random sampling procedure (one-target blocks).

In both-targets blocks, participants were instructed that they were free to fixate either of the target colors. However, to make sure that there would be sufficient switch trials, and that the time between two consecutive switch trials would be long enough for the BOLD response triggered by each of them to not overlap, it was emphasized to participants that the total number of target switches in a block of 40 search displays should roughly be in the range of five to eight. The sampling procedure in one-target blocks then randomly selected (with replacement) a sequence of repeat and switch trials from a pool of sequences that were recorded during both-targets blocks. The motivation behind this was to match one-target blocks and both-targets blocks in terms of switch rate and number of consecutive repeat trials. Importantly, neither features nor positions of the stimuli were replayed but only the sequence of switch and repeat trials. Because we did not yet have any sequences to present at the outset of the experiment, we initialized a pool with four arbitrarily prespecified sequences of switch and repeat trials (one each for five, six, seven, and eight switches per block). To check whether switch rates indeed did not differ between target availability conditions, we ran a paired-samples *t*-test and found a slight, but non-significant difference (both-targets available: 6.4 switches, one-target available: 6.9 switches, $t(18) = 1.9$, $p = .07$, *Cohen's* $d = 0.49$, $BF_{10} = 1$).

Both-targets available and one-target available blocks would differ not only in terms of target availability, but also in the mere number of targets in the display, which would make the one-target available condition more difficult than the both-targets available condition. Therefore, we included trials in the one-target available condition in which there were two target objects, but both carried the same target color, so that still only one target color was present in the search display (*target duplicate*, e.g. on blocks in which red and blue were task-relevant, there could be trials with two red targets or two blue targets, but never with a red and a blue target). In addition, we included trials in which two distractors shared a color (*distractor duplicate*; e.g., on blocks in which red and blue were task-relevant, there could be trials with two green items, but only one red or one blue item), so that participants could not identify the target object simply by detecting a feature duplicate. Likewise, both-targets blocks also contained target duplicate trials (two out of three targets had the same color; e.g., on blocks in which red and blue were task-relevant, we had trials with one red and two blue target objects) as well as distractor duplicate trials (e.g., on blocks in which red and blue were task-relevant, there were trials with one red target, one blue target, and two green distractors). As a result, in each target availability condition, one half of trials contained a target duplicate and the other half contained a distractor duplicate. This way, neither the number of targets nor the number of unique colors in the display was predictive of target availability. Supplementary Table S1 provides schematic representations of all types of search displays. Past experiments using a similar paradigm have confirmed that behavior and ensuing switch costs are consistently unaffected by this manipulation (Ort et al., 2017, 2018), as we also confirm here (see section 3.1). Furthermore, to investigate whether there would be other experimental variables that influenced the choice behavior of the participants we ran a series of control analyses. These analyses are summarized in the Supplementary Material online and Fig. S1.

Because we did not have an eye-tracker available outside of the scanner, participants practiced a version of the task in which target selection responses were made using mouse tracking instead of eye movements (although this naturally involves making an eye movement to the target too). They performed this task before the fMRI session started until they felt confident they understood the task structure. A scanning session consisted of nine functional runs, each 7 min long. One participant requested to terminate the last run early (leaving eight runs of data), while another participant completed ten runs because he expressed the wish to do another run as he liked doing the experiment (data of this run were included). In a single run, both-targets and one-target blocks alternated repeatedly until the end. For the first block in a run, the target availability condition switched relative to the last complete block of the previous run. To make sure that both block types would occur each at least twice per run and that a block would not exceed the run duration, a block was interrupted after 88 s (mean complete block duration = 73 s), or 5 s before the run finished. This resulted in up to five complete blocks per run and, on average, 32 complete blocks per session. Nevertheless, incomplete blocks were still analyzed up to the point of termination.

2.4. Apparatus and functional MRI acquisition

The experiment was designed and presented using the OpenSesame software package (version 3.1.9; Mathôt et al., 2012) in combination with PyGaze (version 0.6), an eye-tracking toolbox (Dalmaijer et al., 2013). Stimuli were back-projected on a screen with a resolution of 1280 × 1024 pixels, at a viewing distance of 60 cm. Participants viewed the screen via an IR-reflecting first surface mirror attached to the head coil. Eye movements were recorded with the EyeLink 1000 remote eye-tracking system, (SR Research, Mississauga, Ontario, Canada) at a sampling rate of 1000 Hz. The experimenter received real-time feedback on system accuracy on a second monitor located in an adjacent room. After every run, eye-tracker accuracy was assessed and improved as needed by applying a 9-point calibration and validation procedure (mean calibration error was 0.48 dva).

Images were acquired using a 3 T Philips Achieva dStream MRI scanner with a 32 channel head coil. Functional images were recorded using a T2*-weighted single-shot gradient echo-planar images sequence with following parameters: 35 axial slices parallel to the AC-PC axis (ascending order), slice thickness = 3 mm, in-plane resolution = 80 × 78 voxels (3 mm × 3 mm), FOV = 240 mm × 240 mm, inter-slice gap of 10% (0.3 mm), whole-brain coverage, TR = 2 s, TE = 30 m s, flip angle = 90°, parallel acquisition with sensitivity encoding (SENSE) with reduction factor 2. After the first five scans were discarded, 210 scans were acquired per functional run. Structural images were recorded using a T1-weighted (T1w) MPRAGE sequence with following parameters: 192 slices, slice thickness = 1 mm, in-plane resolution = 256 × 256 voxels (1 mm × 1 mm), FOV = 256 mm × 256 mm, TR = 9.7 m s, TE = 4.7 m s, inversion time = 900 m s, flip angle = 8°. Distortions of the B0 magnetic field, as well as pulse oximetry and respiratory trace were recorded, but these data were not further processed.

2.5. Eye-tracking data preprocessing

We compared the saccade latencies of eye movements (dwell time before a saccade was executed) for repeat trials (current target category the same as the previous one) with those for switch trials (current target category different from the previous one) for both target availability conditions separately. We took the first saccade after search display onset with an amplitude threshold of 1 dva around initial fixation, provided that a saccade was directed toward the selected target (i.e. its direction deviated less than 30 angular degrees from the vector from fixation to the

target). This resulted in an average of 25.5% of all trials being removed. Note, as we used only the first saccade of a trial and participants needed to select a target before actually fixating it, our paradigm measures covert selection process. Next, a saccade latency filter was applied, in which saccades quicker than 100 m s and slower than 3 standard deviations above the block mean for that participant were excluded (2.2% of all search displays). If no target was being fixated, as could have happened when the eye tracker calibration had deteriorated too much for that trial, both the current as well as the next search display were excluded because neither could be labeled as a switch or repeat (10.6% of all search displays). For the same reason, we excluded the first search display of each block (2.7% of all search displays). If the distance between the stimuli was lowered to prevent the search displays to fall outside the screen, two stimuli could be too close to each other to unambiguously decide which of the two was fixated. Trials on which this happened were also excluded (7.4% of all search displays). In total, 34.4% of all trials were thus removed during preprocessing (note that a single trial could meet multiple exclusion criteria). This is a typical rejection rate for this paradigm (Ort et al., 2017, 2018; van Driel et al., 2019). Inferential statistics were carried out with the *afex* R-package (Singmann et al., 2016).

2.6. Hierarchical drift diffusion modeling

To gain more insight into target selection beyond simple comparisons of mean saccade latencies across conditions, we also performed drift diffusion modeling (DDM) on our data. DDMs can estimate latent decision-related parameters in two-alternative choice experiments based on response time distributions and choice probabilities (Wiecki et al., 2013). For example, participants might be more cautious to respond when only one target is available than when both target colors are present. Similarly, participants might need longer to select a stimulus to fixate on switch trials when only one target is present. In these models, decision-making is assumed to be a noisy information accumulation process in favor of one or the other alternative that continues until a threshold for one option is exceeded and the corresponding response is executed (e.g. Ratcliff and Rouder, 1998). We used a hierarchical Bayesian DDM, as implemented in the python-library *HDDM* (version 0.6; Wiecki et al., 2013), which has the advantage of simultaneously estimating group and individual-subject parameters as well as obtaining a measure for the estimates' uncertainty.

The standard DDM framework provides estimates for four parameters: drift rate v, non-decision time t, boundary separation a, and starting point z (see Fig. 1D). The drift rate represents the speed with which evidence is accumulated during a decision process. It is related to the difficulty of a decision, with hard decisions corresponding to low drift rates and easy decisions to high drift rates. The non-decision time signifies the time needed to encode the stimulus and execute the motor response and is therefore not related to the decision process itself. The boundary separation parameter reflects how much evidence needs to be accumulated before a decision is made, therefore representing response caution (speed-accuracy trade-off). Close boundaries lead to quick and more inaccurate decisions, whereas wide boundaries lead to slower, but more accurate decisions. The starting point denotes whether there is an a priori bias for one of the options.

It has been shown that task repeats are associated with higher drift rates than target switches, plausibly reflecting faster evidence accumulation when a target is repeated (e.g. Karayanidis et al., 2009; Schmitz and Voss, 2012). Based on this finding, we also expected to find higher drift rates for target repeats than for target switches. However, if individuals prepare a target prior to search display onset in both-targets blocks, drift rates for free target switches should likely be higher than for imposed switches, potentially even be as high as the drift rate for target repeats. Furthermore, in Ort et al. (2017), we found base rate differences between both-targets and one-target blocks in terms of saccade latencies: Saccades were generally faster in both-targets blocks than in one-target blocks, irrespective of transition type. This effect might imply strategic differences, such as increased response caution when only one target was available relative to when both were present. To investigate this hypothesis, we estimated a separate boundary separation for both-targets and one-target blocks. As the boundary separation is usually assumed to be under control of individuals and switch and repeat trials were unpredictable in one-target blocks, we did not separately estimate this parameter for repeat and switch trials.

Unlike in standard two-forced choice tasks, there was no single correct or incorrect response in our task. In fact, on every trial, participants could make five possible responses, corresponding to each stimulus (targets and distractors). Therefore, to make our paradigm compatible with the DDM framework, we did not consider individual stimuli as response options, but only distinguished correct (saccades to targets) from incorrect (saccades to distractors) responses. To test our hypotheses about the influence of the experimental conditions on drift rate and boundary separation, we ran four models, in which we manipulated which parameters were free to vary across experimental conditions. These models were: (1) basic model, in which both boundary separation (a) and drift rate (v) were fixed across conditions; (2) decision boundary model, in which a could vary between target availability conditions and v was fixed; (3) drift-rate model, in which v could vary between target availability and transition type conditions, and a was fixed; (4) full model, in which a *and* v could vary between target availability conditions, and v could also vary between transition type condition. We did not estimate intertrial variability of starting point and drift rate in any of the models and fixed the estimate for starting point and non-decision time across conditions, as condition-specific differences in those parameters were implausible. Furthermore, we chose to use informative priors (see Wiecki et al., 2013). Nevertheless, once we identified the best model, we also ran it with non-informative priors as control analysis; the results were virtually identical. Supplementary Table S2 includes the full specifications of all models that were tested.

For every model, 50,000 steps were sampled with Markov Chain Monte Carlo (MCMC). The first 20,000 samples were discarded ("burn in") and only every fifth sample was kept ("thinning") to facilitate convergence. Convergence was tested by visually inspecting all posterior distributions (mc-trace, auto-correlation and marginal posterior histogram) of each parameter, and computing the Gelman-Rubin (R-hat) convergence statistic. The data that were fed into the model were less stringently preprocessed than for the saccade latency analysis. Specifically, neither the first saccade was required to be directed to the eventually fixated target, nor were error trials excluded, because the DDM utilizes both correct and incorrect trials to model reaction time distributions.

The best model was selected based on the lowest deviance information criterion (DIC). Even though the DIC penalizes increased numbers of parameters in a model, it still has a bias to prefer more complex models (Wiecki et al., 2013). Therefore, it should only be used as a heuristic for model selection. Condition-specific differences in the parameters of the selected model were analyzed using a Bayesian approach, that is, we sampled from the posterior distributions of the parameters and compared the likelihood of samples being lower in one condition relative to the other. We considered values larger than 97.5% or smaller than 2.5% significant. Note, even though these posterior probabilities are not the same as confidence intervals, they can be interpreted in a similar way (Wiecki et al., 2013). To test the predictive quality of the model, we compared actual data to simulated data, sampled from the posterior distribution of the fitted model and evaluated the correspondence across several summary statistics.

2.7. Functional MRI preprocessing

FMRI data was preprocessed using FMRIPrep version 1.0.8 (Esteban et al., 2018), a Nipype (Gorgolewski et al., 2011, 2018) based tool. Each T1w volume was corrected for intensity non-uniformity using N4BiasFieldCorrection v2.1.0 (Tustison et al., 2010) and skull-stripped using

antsBrainExtraction.sh v2.1.0 (using the OASIS template). Brain surfaces were reconstructed using recon-all from FreeSurfer v6.0.0 (Dale et al., 1999), and the brain mask estimated previously was refined with a custom variation of the method to reconcile ANTs-derived and FreeSurfer-derived segmentations of the cortical gray-matter of Mindboggle (Klein et al., 2017). Spatial normalization to the ICBM 152 Nonlinear Asymmetrical template version 2009c (Fonov et al., 2009) was performed through nonlinear registration with the antsRegistration tool of ANTs v2.1.0 (Avants et al., 2008), using brain-extracted versions of both T1w volume and template. Segmentation of cerebrospinal fluid (CSF), white-matter (WM) and gray-matter (GM) was performed on the brain-extracted T1w using fast (Y. Zhang et al., 2001) in FSL v5.0.9 (Jenkinson et al., 2002).

Functional data were motion corrected using mcflirt (FSL v5.0.9). "Fieldmap-less" distortion correction was performed by co-registering the functional image to the same-subject T1w image with inverted intensity (Huntenburg, 2014; Wang et al., 2017) and constrained with an average fieldmap template (Treiber et al., 2016), implemented with antsRegistration (ANTs). This was followed by co-registration to the corresponding T1w using boundary-based registration (Greve and Fischl, 2009) with 9 degrees of freedom, using bbregister (FreeSurfer v6.0.0). Motion correcting transformations, field distortion correcting warp, BOLD-to-T1w transformation and T1w-to-template (MNI) warp were concatenated and applied in a single step using antsApplyTransforms (ANTs v2.1.0) using Lanczos interpolation. After the preprocessing with FMRIPrep, functional data were further high-pass filtered at 1/50 Hz using the fslmaths implementation of Nipype.

Physiological noise regressors were extracted applying CompCor (Behzadi et al., 2007). Principal components were estimated for anatomical CompCor (aCompCor). A mask to exclude signal with cortical origin was obtained by eroding the brain mask, ensuring it only contained subcortical structures. For aCompCor, six components were calculated within the intersection of the subcortical mask and the union of CSF and WM masks calculated in T1w space, after their projection to the native space of each functional run. Frame-wise displacement (Power et al., 2014) was calculated for each functional run using the implementation of Nipype. Many internal operations of FMRIPrep use Nilearn (Abraham et al., 2014), principally within the BOLD-processing workflow. See https://fmriprep.readthedocs.io/en/1.0.8/workflows.html for more detail on the pipeline.

2.8. Functional MRI analysis

2.8.1. General linear model

To examine brain activity related to our experimental conditions, we ran an event-related general linear model on the whole brain, separately for each run of each subject. Prior to modeling, functional time series were spatially smoothed with a 5 mm FWHM Gaussian kernel with a nipype implementation of SUSAN (S. M. Smith and Brady, 1997). We separately modeled all combinations of our experimental conditions (both-targets/switch, one-target/switch, both-targets/repeat, one-target/repeat) as well as error trials and the response to the cue display, using display onset times relative to the start of the run as event onset times and the response times as event durations. These events were convolved with a canonical hemodynamic response function (double-gamma), and, together with a number of nuisance regressors, formed the design matrix. Nuisance regressors include the temporal derivative of each event type, motion-related parameters (three regressors each for translation and rotation), framewise displacement (FD), and six anatomical noise regressors (aCompCor). Finally, all volumes with a FD value greater than 0.9 were treated as motion-related outliers and censored, that is effectively excluded from the model. Finally, the data was prewhitened with an autoregressive model to account for temporal autocorrelation (Woolrich et al., 2001). The resulting *t*-statistic maps were combined across runs within participants in a fixed-effect analysis. Next, group analysis was performed with threshold-free cluster enhancement (tfce; S. M. Smith and Nichols, 2009), a voxel-based type statistic that combines the height and spatial extent of local activations. The transformed p-value maps were corrected with nonparametric permutation testing (5000 permutations) as implemented in FSL's *randomise* (Winkler et al., 2014). Finally, the corrected maps were registered to the FreeSurfer surface (*fsaverage*) coordinate system, using registration fusion (Wu et al., 2018). All reported results were initially thresholded at $\alpha = .05$, however, for illustration purposes, activity maps were also thresholded at the more stringent $\alpha = .01$ and shown as overlays (all applied to p-values corrected for multiple comparisons as per above).

2.8.2. Deconvolution

To gain further insight into the time course and extent of the BOLD response as triggered by each event type, we ran a deconvolution analysis in brain regions that are typically considered part of the multiple-demand (MD) network, that has been associated with cognitive control in a variety of contexts (Duncan, 2010; Fedorenko et al., 2013), plus showed generic switch-related activity in our GLM analysis. To do this, we first converted the preprocessed functional data to represent the percent signal change of the time series, concatenated them across runs and averaged the resulting series within each region of interest (ROI). We defined ROIs based on an existing set of masks of MD subregions (Fedorenko et al., 2013). These ROIs were then combined with voxels that showed significant switch-related activity (collapsed over target availability) in our GLM analysis, yielding 23 ROIs in total. The deconvolution was performed with nideconv (de Hollander and Knapen, 2018). We used the same regressors as in the GLM analysis with the exception that the temporal derivative regressors were not included. All other regressors were convolved with a Fourier basis set, comprising an intercept and four sine-cosine pairs. Prior to estimation, the design matrix was oversampled 20-fold to improve the temporal resolution. For each regressor, beta weights were estimated with ridge regression for each participant separately. The deconvolved time series were extracted from the beta weights and averaged across participants. To statistically test for significant activations, we used a permutation test with 1000 permutations (MNE - one-sample *t*-test; Gramfort et al., 2013) and a cluster-based approach to correct for multiple comparisons. Finally, to test for potential onset differences between proactive and reactive switch-related activity, we used fractional peak latency in combination with the jackknife approach (Liesefeld, 2018; Luck, 2014; Miller et al., 1998). In doing so, we averaged the deconvolved time series of all but one participant and identified the time point at which the time series reached 50% of the peak, separately for the proactive and the reactive conditions. To mitigate the influence of local extreme values on the latency estimation, for every time point we averaged the amplitude over five time consecutive points (centered at the current time point). We repeated this procedure leaving out each participant once and computed a paired-sample *t*-test over the onset estimates. To correct for the artificially reduced error term in the jackknife approach, we followed Miller et al. (1998) by effectively dividing the *t*-statistic by the degrees of freedom.

3. Results

3.1. Behavioral results

We observed switch costs (longer saccade latency after target switches than target repetitions) only in one-target available blocks but not in both-targets available blocks (Fig. 1B and C). This was statistically confirmed by a two-way repeated-measures ANOVA with target availability (both-targets available vs. one-target available) and transition type (repeat vs. switch) as factors on saccade latency. This ANOVA revealed significant main effects of target availability ($F(1, 18) = 18.3$, $p < .001$, $\eta^2 = .50$) and transition type ($F(1, 18) = 23.3$, $p < .001$, $\eta^2 = .56$), and a significant interaction between them ($F(1, 18) = 16.7$, $p < .001$, $\eta^2 = .48$). A Bayes Factor analysis confirmed this pattern by showing that the model including both main effects and the interaction

effect explains the data best ($BF = 7.8 \times 10^5$) and was 12.2 times as likely as the next best model including only the main effects. Overall, saccade latencies were lower in both-targets blocks than in one-target blocks, and lower on switch trials than on repeat trials. Critically however, significant switch costs emerged only in one-target blocks (target repeat: 388 m s vs. target switch: 452 m s; $t(18) = 5.1$, $p < .001$, *Cohen's* $d = 0.63$), and not on both-targets blocks (target repeat: 374 m s vs. target switch: 388 m s; $t(18) = 2.0$, $p = .06$, *Cohen's* $d = 0.20$). Bayesian t-tests confirmed this conclusion by providing very strong evidence for the presence of switch costs in the one-target condition ($BF_{SwitchCosts} = 374$), but no conclusive evidence for either the presence of absence of switch costs in the both-targets condition ($BF_{SwitchCosts} = 1.2$).

Next, we analyzed fixation accuracy, that is, the proportion of trials on which participants fixated a target relative to all trials (see Table 1). The data pattern here confirms the saccade latency results with switch costs in one-target blocks and no switch costs in both-targets blocks, precluding an interpretation in terms of a speed-accuracy tradeoff. To test these results, we ran a two-way repeated measures ANOVA with the same factors on accuracy, which also yielded significant main effects of target availability ($F(1, 18) = 42.6$, $p < .001$, $\eta^2 = .70$) and transition type ($F(1, 18) = 37.8$, $p < .001$, $\eta^2 = .68$), as well as a significant interaction between them ($F(1, 18) = 28.6$, $p < .001$, $\eta^2 = .61$). Again, this was supported by a Bayes Factor analysis indicating that the full model ($BF = 1.8 \times 10^{10}$) is 1746 times more likely than the model with only main effects ($BF = 1.8 \times 10^7$).

Finally, to test whether the different display types (target duplicate vs. distractor duplicate) had an influence on the presence or absence of switch costs in each target availability condition, we ran a three-way repeated measures ANOVA with target availability, transition type and display type as factors on saccade latency. However, neither the main effect display type, nor any of the interactions that included that term were significant ($p > .12$). The full ANOVA results can be found in the supplementary material online.

3.2. Hierarchical drift diffusion modeling results

Of all models that we ran (see Table S2), the full model with a variable drift rate for target availability and transition type and a variable boundary separation for target availability performed best in explaining the data, as indicated by the lowest DIC (-5.15×10^5). The next best model was the drift-rate-only model with a DIC of -5.13×10^5. We estimated the posterior probability distributions for the condition-specific drift rates and boundary separations and tested for significance directly on the posterior distributions (see Fig. 1E). Using the posterior probabilities, we examined how likely it would be for parameter estimates to be greater in one condition compared to another (P[X > Y]). For drift rates, we compared switch to repeat trials in both target availability conditions separately. Drift rates were significantly higher in repeat trials than in switch trials for one-target blocks (switch: $v_{mean} = 2.31$, repeat: $v_{mean} = 3.70$, P[switch > repeat] = 0%). In both-targets blocks drift rates were also higher for repeat trials than for switch trials, but the difference was not as large (switch: $v_{mean} = 3.88$, repeat: $v_{mean} = 4.22$, P[switch > repeat] = 9%). This suggests that participants needed more time to decide whenever selecting a different target than on the previous trial, particularly when only one target was available. Nevertheless, the higher likelihood for drift rates to be larger for repeat than switch trials when both targets were present suggests that also in this condition, some switch-related cost was present. Even though the best model included separate estimates for boundary separation for one-target blocks and both-targets blocks, comparing these boundary separation estimates to each other yielded virtually the same value (one-target available: $a_{mean} = 1.17$, both-targets available: $a_{mean} = 1.16$, P[both-targets > one-target] = 47%). This suggests that participants did not adjust their response caution across target availability conditions. This finding is somewhat unintuitive given that the best model included a separate boundary separation parameter for each target availability condition, but could be caused by the DIC being biased toward the more complex model (see Wiecki et al., 2013). Finally, to confirm that the full model accurately captured the data, we examined the quality of the model fit. In addition, we also checked whether the simpler drift-rate-only model (only drift rate could vary across experimental conditions) was also representative of the data, we analyzed that model as well. For this purpose, we generated data by sampling from the posterior distributions of the parameters and compared the simulated data to the original data. Importantly, key summary statistics, such as accuracy, mean, median, quantiles (10, 30, 50, 70, 90) saccade latencies, were all recovered in the simulated data, as indicated by all summary statistics lying within the 95% credible intervals. This indicates that both models provide a good fit to the data and interpreting their parameters is warranted.

Table 1
Percentage correctly fixated targets for all conditions in all three experiments with within-subject 95% confidence intervals (Morey, 2008).

Target Availability	Target Switch	Target Repeat
Both-Targets	96.1 [95.4, 97.0]	96.9 [96.2, 97.6]
One-Target	87.2 [85.4, 89.0]	95.3 [94.6, 96.0]

3.3. Neuroimaging results

3.3.1. General linear model

To determine whether the behavioral effects in terms of switch costs are governed by separable cognitive control mechanisms, we used a general linear model (GLM) to examine whether BOLD activity associated with updating a target representation depended on how many unique targets were available in a search display. Before comparing switch-related activity across target availability conditions, we first contrasted switch trials with repeat trials, separately within the one-target and the both-targets condition. When both targets were available, switches elicited widespread activations across cerebral cortex and cerebellum, in a network reminiscent of the multiple-demand (MD) network (see Fig. 2 and Table 2). Bilateral frontal activations include dorsolateral prefrontal cortex (dlPFC), frontopolar cortex, dorsal premotor cortex (PMd), inferior frontal junction (IFJ), anterior insula/frontal operculum cortex (aINS), posterior cingulate gyrus (pCG), and medial frontal cortex (spanning from the dorsal anterior cingulate cortex to the frontal eye fields, mFC/dACC). Parietal activations were found bilaterally in the superior parietal lobule (SPL), extending across the intraparietal sulcus (IPS) into the inferior parietal lobule (IPL), including supramarginal and angular gyrus. In the occipital and temporal lobe, there was switch-related activity in the intracalcarine sulcus and in temporo-occipital regions, bilaterally and in the right inferior temporal gyrus. Finally, several subregions in the cerebellum were activated as well. When only one target was available, fewer significant clusters were found (see Fig. 3 and Table 2). Activations were restricted primarily to posterior regions in the parietal and occipital lobe, including IPS, SPL, and IPL as well as the cerebellum. However, two smaller activated regions were also found in the left IFJ, and the dlPFC at the border with the frontopolar cortex.

Next, to statistically compare switch-related activity between target availability conditions, we directly compared activity associated with each target availability condition to each other. However, because target availability was manipulated at the block-level, when directly comparing switch-related activity across target availability conditions, we might pick up on overall block differences rather than true switch-related differences. We therefore computed a double contrast, in which we first isolated switch-related activity per target availability condition by subtracting repeat activity from switch activity, and next, contrasted these differences to obtain the neural correlate of switching when both targets were available versus when one target was available. When considering regions where switch-related activity was stronger in both-targets blocks than in one-target blocks, we again found activations closely resembling

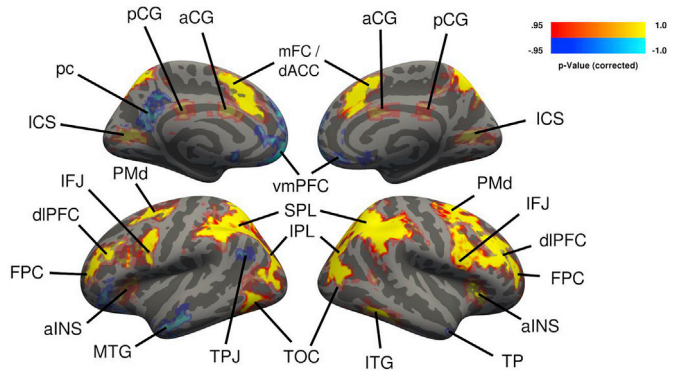

Fig. 2. Cerebral activations for the free choice condition (proactive control demand). Activations shown in yellow-red represent the contrast free switch > free repeat; activations shown in blue represent the contrast free repeat > free switch. Group-level *t*-statistics maps were computed with the tfce-method (S. M. Smith and Nichols, 2009) and corrected for multiple comparisons using nonparametric permutation testing. The resulting P-value maps were thresholded at $\alpha = .05$ and projected onto the fsaverage surface using registration fusion (Wu et al., 2018), with translucent coloring. In addition, regions that were also significant at $\alpha = .01$ are shown in saturated colors. Free switches were associated with higher activity than free repeats across both hemispheres in dorsolateral prefrontal cortex (dlPFC), frontopolar cortex (FPC), dorsal premotor cortex (PMd), inferior frontal junction (IFJ), anterior insula/frontal operculum cortex (aINS), posterior cingulate gyrus (pCG), anterior cingulate gyrus (aCG), medial frontal cortex (spanning from the dorsal anterior cingulate cortex to the frontal eye fields, mFC/dACC), superior parietal lobule (SPL), inferior parietal lobule (IPL), intracalcarine sulcus (ICS), right inferior temporal gyrus (ITG), temporo-occipital cortex (TOC), and bilateral cerebellum (not shown here). Free repeats were associated with higher activity than free repeats in the left precuneus (pc), bilateral ventromedial prefrontal cortex (vmPFC), left medial temporal gyrus (MTG), left temporoparietal junction (TPJ) and right temporal pole (TP).

the MD network, including bilateral dlPFC, frontopolar cortex, mFC/dACC, pCG, SPL, IPS, and Cerebellum (Fig. 4). The opposite contrast –more switch-related activity in the one-target condition than in both-targets available condition– yielded no significant activations. One possibility might be that in the one-target condition, target representations often needed to be updated both on switch and repeat trials, for example if participants did not anticipate any of the targets. If this is the case, switch and repeat trials would be more similar in the one-target available condition, so that activity reflecting switch costs would be reduced.

To investigate this possibility, we directly compared switch activations between target availability conditions without taking repeat events into account (see Fig. S2). For the contrast both-targets switch greater than one-target switch, a very similar pattern was found as in the double-contrast analysis (only bilateral aINS and Caudate were additionally active), thus confirming the previous findings and suggesting that block differences do not seem to play an important role. More importantly, when considering the opposite contrast, significant clusters of activation were now found in the left ventrolateral prefrontal cortex (vlPFC), precuneus, and left temporoparietal junction, regions that have been considered part of the default mode network (DMN; Raichle, 2015; Raichle et al., 2001). The DMN has recently been linked to automated behavior, not rigorously governed by cognitive control (Vatansever et al., 2017). Therefore, stronger DMN activations in one-target blocks could be explained by less control being applied during switches in this condition compared to both-targets blocks. If so, the same should be true for repeat trials. For this reason, these DMN activations might not have emerged in the double-contrast procedure, as these activations canceled each other out when switch and repeat trials in the one-target condition were contrasted with each other. To investigate whether there actually was DMN activity associated with repeat trials, in an exploratory analysis, we examined whether there were regions in which repeat events led to

Table 2
Localization of activations for the main contrasts. Coordinates of local maxima are reported in MNI152-space. Large clusters were split into subclusters based on anatomical considerations. Structure labels are based on the Harvard-Oxford anatomical atlas.

Structure	t-statistic	X	Y	Z
Proactive Switch > Proactive Repeat				
Left Anterior Insula	8.26	−33	21	8
Right Anterior Insula	8.24	33	24	8
Left Precentral Gyrus/Inferior Frontal Junction[c]	8.25	−45	0	38
Right Precentral Gyrus/Inferior Frontal Junction[c]	6.95	52	8	25
Left Middle Frontal Gyrus/Dorsal Premotor Cortex[c]	7.58	−27	−6	54
Right Middle Frontal Gyrus/Dorsal Premotor Cortex[c]	8.41	27	12	47
Superior Frontal Gyrus/Medial Frontal Gyrus[c]	8.31	0	18	47
Posterior Cingulate Gyrus	7.69	0	−30	28
Left Intraparietal Sulcus[b]	9.35	−30	−54	44
Right Intraparietal Sulcus[b]	9.27	36	−45	41
Left Inferior Parietal Lobule	8.99	−30	−75	27
Right Superior Parietal Lobule	8.92	39	−63	61
Right Intracalcarine Sulcus	6.19	24	−72	8
Left Intracalcarine Sulcus	6.16	−18	−66	5
Left Cerebellum (Crus I)[a]	8.9	−33	−63	−32
Right Cerebellum (Crus I)[a]	8.75	36	−57	−32
Proactive Repeat > Proactive Switch				
Medial Frontal Cortex	7.08	−3	57	−9
Left Orbitofrontal Cortex	6.62	−39	36	−15
Right Orbitofrontal Cortex	5.36	33	39	−15
Subcallosal Gyrus	5.88	0	15	−9
Medial Frontopolar Cortex	5.64	0	60	19
Right Temporal Pole	6.35	51	15	−32
Left Middle Temporal Gyrus	5.99	−60	0	−25
Left Inferior Parietal Lobule/Temporoparietal Junction[c]	6.18	−45	−57	24
Precuneus	6.13	−6	−54	21
Reactive Switch > Reactive Repeat				
Left Lateral Frontopolar Cortex	5.28	−42	39	11
Left Precentral Gyrus/Inferior Frontal Junction[c]	5.04	−42	0	34
Left Intraparietal Sulcus[b]	6.76	−30	−51	44
Right Intraparietal Sulcus[b]	6.21	36	−45	41
Left Fusiform Gyrus	5.55	−33	−54	−19
Cerebellum (Vermis VI)[a]	5.74	6	−72	−25
Right Cerebellum (Crus I)[a]	5.67	33	−54	−35
Left Cerebellum (Crus I)[a]	5.16	−39	−51	−35
Reactive Repeat > Reactive Switch				
Medial Frontal Cortex	7.69	0	45	−12
Medial Frontopolar Cortex	6.07	−4	58	4
Left Temporal Pole	5.61	−48	9	−35
Right Amygdala	4.53	15	−9	−15
Left Amygdala	3.98	−15	−7	−16
Left Hippocampus	6.51	−24	−21	−15
Right Hippocampus	4.42	24	−24	−12
Left Precuneus	6.29	−15	−48	34
Left Inferior Parietal Lobule/Temporoparietal Junction[c]	5.88	−57	−69	31
Proactive Switch Cost > Reactive Switch Cost				
Right Lateral Frontopolar Cortex	7.59	48	42	24
Left Lateral Frontopolar Cortex	6.5	−36	63	18
Right Middle Frontal Gyrus/Dorsal Premotor Cortex[c]	7.47	24	15	47
Right Middle Frontal Gyrus	6.04	51	30	38
Superior Frontal Gyrus/Medial Frontal Gyrus[c]	6.11	3	21	51
Posterior Cingulate Gyrus	5.27	0	−33	28
Right Superior Parietal Lobule	7.59	42	−60	61
Right Intraparietal Sulcus[b]	5.61	33	−51	40
Left Intraparietal Sulcus[b]	5.08	−30	−57	50
Left Cerebellum (Crus I)[a]	6.65	−36	−63	−32
Right Cerebellum (Crus I)[a]	5.08	36	−57	−32

[a] These structure labels were retrieved from the Probabilistic cerebellar atlas (included in FSL).
[b] These structure labels were retrieved from the Juelich Histological Atlas.
[c] Additional labels were provided to further specify anatomical location or functional significance.

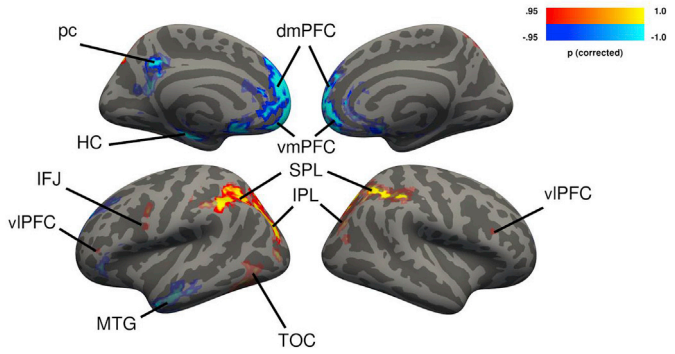

Fig. 3. Cerebral activations for the imposed choice condition (reactive control demand). Activations shown in yellow-red represent the contrast imposed switch > imposed repeat; activations shown in blue represent the contrast imposed repeat > imposed switch. Group-level *t*-statistics maps were computed with the tfce-method (S. M. Smith and Nichols, 2009) and corrected for multiple comparisons using nonparametric permutation testing. The resulting P-value maps were thresholded at α = .05 and projected onto the fsaverage surface using registration fusion (Wu et al., 2018), with translucent coloring. In addition, regions that were also significant at α = .01 are shown in saturated colors. Imposed switches were associated with higher activity than imposed repeats bilaterally in dorsolateral prefrontal cortex (dlPFC), left inferior frontal junction (IFJ), superior parietal lobule (SPL), inferior parietal lobule (IPL), temporo-occipital cortex (TOC), and bilateral cerebellum (not shown here). Imposed repeats were associated with higher activity than imposed repeats in the left precuneus (pc), bilateral ventromedial (vmPFC), dorsomedial prefrontal cortex (dmPFC), left medial temporal gyrus (MTG), and left hippocampus (HC).

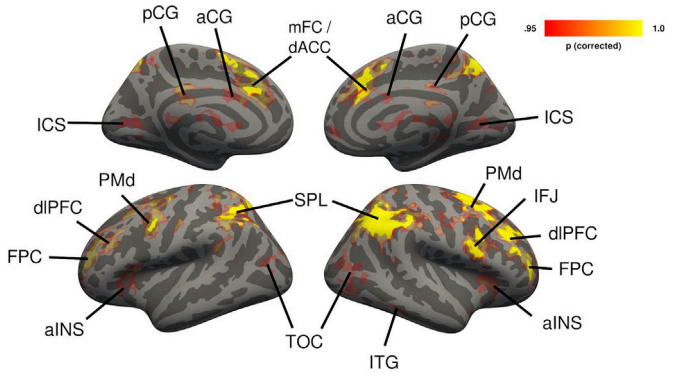

Fig. 4. Cerebral regions in which free switch cost (free switch > free repeat) yielded stronger activity than imposed switch cost (imposed switch > imposed repeat), shown in yellow-red. Group-level *t*-statistics maps were computed with the tfce-method (S. M. Smith and Nichols, 2009) and corrected for multiple comparisons using nonparametric permutation testing. The resulting P-value maps were thresholded at α = .05 and projected onto the fsaverage surface using registration fusion (Wu et al., 2018), with translucent coloring. In addition, regions that were also significant at α = .01 are shown in saturated colors. Free switch costs were associated with higher activity than imposed switch cost across both hemispheres in dorsolateral prefrontal cortex (dlPFC), frontopolar cortex (FPC), dorsal premotor cortex (PMd), inferior frontal junction (IFJ), anterior insula/frontal operculum cortex (aINS), bilateral posterior cingulate gyrus (pCG), anterior cingulate gyrus (aCG), medial frontal cortex (mFC/dACC), superior parietal lobule (SPL), intaparietal sulcus (IPS), intracalcarine sulcus (ICS), right inferior temporal gyrus (ITG), temporo-occipital cortex (TOC), and bilateral Cerebellum (not shown here).

stronger activation than switch events, separately for the both-targets and one-target conditions.

In this exploratory analysis, we effectively reversed the contrast that was used to isolate switch-related activity in the first step of the double contrast procedure. We indeed detected strong activity along the medial wall of the PFC, the orbitofrontal cortex (OFC), the precuneus, the left medial temporal gyrus (MTG), and the temporoparietal junction (TPJ) across both target availability conditions (opposite contrast shown in blue in Figs. 2 and 3). In addition to these common activations, the amygdala and the hippocampus were selectively active in the one-target blocks (Fig. 3). Directly comparing both-targets to one-target repeat trials (not taking switch trials into account), yielded three cluster in which there was stronger activity in the one-target condition. These clusters were located in the precuneus, the medial PFC, MTG, and the TPJ (Fig. S3). The opposite contrast did not show any significant activations, suggesting that the DMN was activated more strongly when one target was available than when both targets were available, which could indicate a higher demand for cognitive control during both-targets blocks than during one-target blocks (see Discussion), or conversely, more automated behavior during the latter. To test this hypothesis, finally, we compared activity between target availability conditions across all event types (collapsed across transition type). This analysis indicates primarily DMN activity (precuneus, vlPFC, TPJ, and medial PFC) in one-target blocks and MD network activity (bilateral dlPFC, aINS, PMd, IFJ, frontopolar cortex, mFC/dACC, SPL) in both-targets blocks (Fig. S4), in line with the hypothesis that more control is demanded during both-targets blocks.

Taken together, the GLM findings demonstrate that for both-targets as well as one-target switches, activations were found in what is known as the multiple-demand network. However, these activations were stronger and more widespread for free switches than for imposed switches. Furthermore, during repeat trials, the DMN was strongly active, particularly during one-target blocks. Irrespective of transition type (switch versus repeat), the MD network seems to be more engaged when both targets are available than when only one is there, in which case the DMN is predominantly active.

3.3.2. *Deconvolution analysis*

The standard approach of modeling the BOLD response with a canonical hemodynamic response function (HRF) maximizes sensitivity for activations at the expense of being more biased towards a predefined shape of the response (Poldrack et al., 2011). To characterize potential interregional variability and accommodate non-standard BOLD-responses not captured by the double-gamma function that we used in the GLM approach, we employed a deconvolution analysis. Deconvolution has the advantage that the shape and the time course of the HRF can vary and some temporal information can be retained. We limited this analysis to ROIs that are part of the MD network and showed switch-related activity (collapsed across target availability) in the GLM (see section 2.8.2), to limit the number of analyses, while still considering most regions in which switch-related activity might be found. Across both cerebral cortex and cerebellum, 23 ROIs were considered. We focused on activation differences between imposed and free switches, specifically where the activation patterns diverge from the standard GLM results described above. Such differences were found primarily for imposed switches. Specifically, the deconvolution identified significant activity bilaterally in the anterior Insula (aINS) and the left dorsal premotor cortex (PMd) located on the superior frontal gyrus. Nevertheless, in these regions, free switches still elicited a stronger response than imposed switches (see Fig. 5). Across all other ROIs, we observed four patterns: regions with neither imposed nor free switch activity, regions with only free switch activity, regions with both imposed and free switch activity but more activity on free switches, and regions with equal amounts of imposed and free switch activity. However, in all those regions the deconvolution yielded the same qualitative pattern as the standard GLM approach.

Note that beyond regional differences between imposed and free

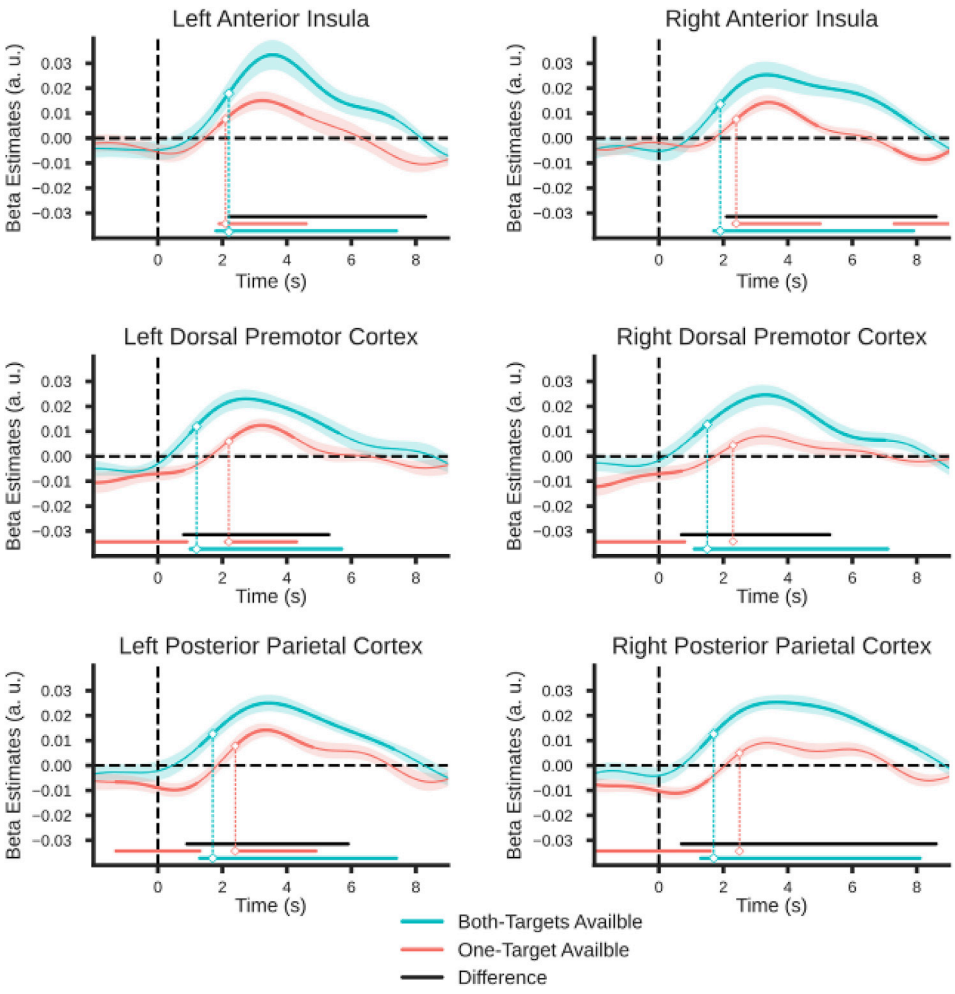

Fig. 5. Group-averaged beta estimates of neural activation time course in selected regions of interest. Deconvolution analysis was used to model the BOLD response for each event type separately. For each target availability condition, the difference of the time courses for switch and repeat trials was computed and the resulting time courses are shown here. The shaded color bands represent 68% confidence intervals (±1 SEM). Thick lines as well as horizontal bars indicate significant clusters (at α = .05) as produced by cluster-based permutation testing (5000 permutations). The black horizontal bars indicate the range over which the difference between the target availability condition was significant. The marked time points (vertical dashed lines) indicate the latency of 50% maximum amplitude as estimated using a jackknife approach, as a measure of the onset of activation (Miller et al., 1998; Luck, 2014; Liesefeld, 2018).

switches, these two conditions could also differ in temporal aspects. In fact, a strong prediction of the dual mode of control framework is that proactive control should begin before trial onset, whereas reactive control should only be invoked after the search display onset. van Driel et al. (2019) provided strong support for this prediction using a very similar paradigm to ours in combination with more time-sensitive EEG measures. To test for potential onset differences also in the fMRI signal, we measured the estimated onset latency in combination with a jackknife approach. The results yielded significantly earlier proactive switch activity in the left PMd ($M_{proactive} = 1210$ m s, $M_{reactive} = 2237$ m s, $t_c(18) = 2.77$, $p_c = .01$), right PMd ($M_{proactive} = 1484$ m s, $M_{reactive} = 2300$ m s, $t_c(18) = 2.53$, $p_c = .02$), left IFJ ($M_{proactive} = 1484$ m s, $M_{reactive} = 2226$ m s, $t_c(18) = 2.79$, $p_c = .01$), right IFJ ($M_{proactive} = 1505$ m s, $M_{reactive} = 2000$ m s, $t_c(18) = 2.99$, $p_c = .008$), left posterior parietal cortex ($M_{proactive} = 1721$ m s, $M_{reactive} = 2405$ m s, $t_c(18) = 2.22$, $p_c = .04$), right posterior parietal cortex ($M_{proactive} = 1747$ m s, $M_{reactive} = 2516$ m s, $t_c(18) = 3.33$, $p_c = .004$), and mFC/dACC ($M_{proactive} = 1284$ m s, $M_{reactive} = 2026$ m s, $t_c(18) = 2.79$, $p_c = .01$), but no such difference in the bilateral aINS (left: $M_{proactive} = 2152$ m s, $M_{reactive} = 2115$ m s, $t_c(18) = 0.41$, $p_c = .69$; right: $M_{proactive} = 1900$ m s, $M_{reactive} = 2410$ m s, $t_c(18) = 1.50$, $p_c = .15$). Some of these areas, notably mFC/dACC and PMd, are consistent with the midfrontal topography of the free choice related beta-oscillatory suppression that was observed by van Driel et al. (2019). Note that one might also expect to find onset differences in the frontopolar cortex, given its presumed role in voluntary switching (Mansouri et al., 2017; Pollmann, 2016). However, as there was virtually no activity related to imposed switches in this region, onset difference could not meaningfully be determined.

4. Discussion

In this study we set out to examine which brain regions are recruited in multiple-target search, depending on whether observers are free to select a target or whether they are forced to select a particular target. For this purpose, we asked observers to look for multiple targets and we manipulated whether both or only one of the two potential target colors were present in a search display. We reasoned that the presence of both targets would enable observers to use proactive control to prepare a search, whereas the presence of only a single item would require reactive control whenever the observer expected the wrong target. In accordance with previous findings (Ort et al., 2017, 2018), we found clear switch costs in terms of both saccade latency and saccade accuracy when only one target category was present in a search display, while there were no switch costs when both targets were available. This finding is further supported by the results of hierarchical drift diffusion modeling, which revealed lower drift rates on switch compared to repeat trials when one target was available. When both targets were present, drift rates were also lower for switch than for repeat trials, but this difference was much smaller than in the one-target condition. This suggests that observers used the predictability of the both-targets condition to prepare selection of either one of the targets, so that potential costs associated with updating the currently active target representations remained latent.

Importantly, using fMRI measures we provide new evidence regarding the neural mechanisms underlying these switches of feature-based attention. We found the frontoparietal multiple-demand network

(Duncan, 2010; Fedorenko et al., 2013) to be strongly associated with free target switches. Imposed target switches elicited a similar, yet weaker activity pattern in the posterior parietal cortex (PPC), and relatively smaller activity clusters in frontal regions at the inferior frontal junction (IFJ) and dorsolateral prefrontal cortex (dlPFC). Furthermore, the direct comparison of free and imposed switches indicates that the multiple-demand network is more strongly involved during free than during imposed switches. In contrast, parts of the default mode network are activated stronger in blocks involving imposed switches. Assuming that target availability conditions primarily differed with respect to whether observers used proactive control (both-targets available) or reactive control (one-target available), our findings suggest that these two modes of control can indeed be dissociated during multiple-target search. More specifically, by means of a deconvolution analysis, we were able to categorize these differential activations into regions that exclusively activate for free switches (dlPFC, frontopolar cortex, and medial frontal cortex/mFC) and regions that are also active during imposed switches but to a lesser extent (IFJ, dorsal premotor cortex/PMd, and PPC). Furthermore, these regions activated earlier for free switches, corroborating their role in preparatory cognitive control in anticipation of a demanding event.

The observed activations for imposed switches are reminiscent of earlier reports on stimulus or task-induced feature-based attention shifts with activations primarily located bilaterally in PPC and PMd (Greenberg et al., 2010; Liu et al., 2003; Pollmann et al., 2006, 2000, Slagter et al., 2006, 2007). This also matches the observation that IFJ and PPC are involved in updating and representing task sets across a variety of tasks (Brass and von Cramon, 2004; Kim et al., 2012). In particular, it has been suggested that while IFJ is responsible for updating task-specific information, the PPC maintains such information and implements task sets (Brass and von Cramon, 2004; Bunge et al., 2003; Greenberg et al., 2010; Shulman, 2002; Slagter et al., 2007). Finally, the activity in the anterior insula that we observed after deconvolution analyses of both types of switches may be part of a network that signals salient events (such as the absence of an expected target color) and the need to initiate a cascade of control signals that eventually update the active target representation (Menon and Uddin, 2010; Power and Petersen, 2013; Seeley et al., 2007). We isolated the neural response to feature-based attention shifts from the additional types of changes that may contribute to task-switch costs (e.g. Meiran, 2010), in particular shifts of stimulus-response mapping. Our findings suggest that establishing a new attentional set is a rather "cheap" process that requires only minimal frontal activity (see Ort et al., 2019; Moore and Weissman, 2010 for behavioral and electrophysiological evidence). Furthermore, similar to Gmeindl et al. (2016), we directly compared endogenous, self-initiated target switches to imposed switches, but of feature-based rather than spatial attention. Importantly, our design allowed us to link either switch-related activity to specific events in the experiment. In doing so, we show that there is common, but also distinct neural activity underlying these types of switches.

However, some findings were unexpected, in particular with respect to imposed switches. First, with the standard GLM approach, we did not observe any significant imposed-switch-related activity in the dorsal premotor cortex (PMd; presumably the location of the human frontal eye fields), an area that has previously been shown to be related specifically to feature-based attention shifts (Kim et al., 2012). Using deconvolution, we were able to detect significant, but relatively weak activity in the left PMd. A possible explanation may be that in contrast to earlier studies of feature-based attention shifts (e.g. reviewed in Kim et al., 2012), in our study, there were no changes in the stimulus-response mapping associated with imposed switches. Note that an imposed target shift did not systematically signal a particular eye movement as target location and target identity were unrelated. Therefore, there was no need to activate or update a certain stimulus-response mapping, which has been suggested to be a function of the PMd (e.g. Badre and D'Esposito, 2009; Hopfinger et al., 2000; Kim et al., 2012). This is also supported by Pollmann et al. (2006), who, during a visual search task, separated attention shifts from response shifts and found only the latter to activate the PMd.

Second, unlike Jiang et al. (2018), we did not observe any activity in the anterior cingulate cortex (ACC) related to imposed switches. This region has been linked to conflict monitoring in numerous studies (e.g. Botvinick et al., 1999; Ito et al., 2003; Jiang et al., 2015; Kerns et al., 2004; Ullsperger et al., 2014). As observers could not anticipate imposed target switches, we also expected a degree of surprise whenever the target changed. This signal has been suggested to be related to conflict-processing and to originate in the medial frontal cortex (e.g. Cavanagh and Frank, 2014). However, experienced conflict in Jiang et al. (2018) may have been stronger due to the fact that participants were explicitly cued as to which task to expect, while in our study any build-up of expectations was left to the observer. Furthermore, unlike in the Jiang et al. study, observers did not have to manage a target-specific stimulus-response mapping in our study. Overall, we believe that target selection in our paradigm was relatively easy and therefore did not evoke strong conflict-related signals in the frontal cortex. That said, in a recent EEG study with a very similar paradigm (van Driel et al., 2019), we did observe a power enhancement in the delta/theta-frequency band after imposed switches over midfrontal electrodes. This signal has been suggested to be related to conflict-processing and to originate in the medial frontal cortex (e.g. Cavanagh and Frank, 2014). It remains to be investigated why we found no corresponding source here.

Some support for the hypothesis that relatively little control was exerted in the imposed target condition comes from the default mode network activity that we observed, particularly for repeat trials. The default mode networkhas recently been shown to not just reflect an idle brain state, but to also activate during various tasks (Elton and Gao, 2015; Konishi et al., 2015; Smallwood et al., 2013; V. Smith et al., 2018; Spreng, 2012; Spreng et al., 2014; Vatansever et al., 2017). Even though its functional significance is still debated, there is increasing evidence that suggests the default mode network is related to internally-generated thought (Konishi et al., 2015), decoupled from immediate sensory input or context-representation (V. Smith et al., 2018). Maybe most importantly, Vatansever et al. (2017) demonstrated that even though the cognitive control network is strongly involved in acquiring task rules, once those rules have been learned, the default mode network becomes active while applying them. They concluded that whenever the current task context is predictable, individuals enter a form of "autopilot" mode in which correct responses can be made without explicit cognitive control. We argue the same may happen in our paradigm: During phases of target repeats, participants were able to select the correct target disk in a low-control, automated manner.

The activation patterns associated with free switches are similar to previously reported activations related to proactive control demand (Irlbacher et al., 2014; Jiang et al., 2018). In addition to parietal and posterior frontal activity as was also observed for imposed switches, two key activations are of primary importance here. First, there were strong medial activations spanning from dorsal anterior cingulate cortex (dACC) to the supplementary motor area (SMA). Activity in these regions has been associated with self-generated choice (Demanet et al., 2013; Forstmann et al., 2006; Gmeindl et al., 2016; Orr and Banich, 2013; Passingham et al., 2010; Soon et al., 2008; Taylor et al., 2008; Wisniewski et al., 2016; Wisniewski et al., 2015; J. Zhang et al., 2013). The present pattern of activations matches those findings, consistent with the idea that participants used the available information to prepare a switch trial in advance. Second, activity was found in the lateral frontopolar cortex. This region has been associated with making free decisions, but also with the evaluation of alternative goals in the context of exploratory behavior (Mansouri et al., 2017; Pollmann, 2016). We believe that this activity might reflect participants evaluating whether or not to switch to the other target color during a streak of target repeats. Nevertheless, even though these activations were specific to the free choice condition, they may only indirectly relate to proactive control, inasmuch as this information can be used by a cognitive control system to signal when (and supposedly how much) proactive control should be invoked.

In addition, we also found activity along the dlPFC. In line with an interpretation in terms of proactive control, this activity might reflect preparatory updating and maintaining of task rules (Braver et al., 2009). However, as the dlPFC has been linked to a wide range of executive functions, such as working memory, planning, and inhibition (e.g. Niendam et al., 2012), we cannot exclude that other factors caused the activations in this region. For example, dlPFC activity could have been caused by additional mental effort and working memory demand associated with overall planning or keeping track of the switches, in order to adhere to the task instructions (e.g. Braver et al., 1997; Bunge et al., 2001; Dosenbach et al., 2008; Rypma and D'Esposito, 1999; Shenhav et al., 2013). Nevertheless, it could be argued such additional cognitive processes, despite not being cognitive control in a strict sentence, are essential for proactive control. In this sense, proactive control requires the maintenance of the current and the targeted state (working memory), planning target selection on future trials (planning) and making the decision to invoke proactive control at a given moment (intention). Therefore, the actual usage of proactive control can be seen as a consequence of an cascade of other cognitive processes.

Beyond that, the present findings provide further support for multiple-state models of working memory postulating that the number of memory items that can concurrently affect behavior at any given moment is limited (Huang and Pashler, 2007; Oberauer, 2002; Olivers et al., 2011). The fact that we observed switch costs indicates that observers did not distribute resources equally across multiple target representations. This interpretation is supported by the fMRI results which show switch-related activity in both target availability conditions in regions that have previously been associated with updating of attentional sets (Greenberg et al., 2010; Liu et al., 2003; Pollmann et al., 2006, 2000; Slagter et al., 2006, 2007; Wager et al., 2004), including bilateral posterior parietal cortex and inferior frontal junction. Switch-related activity in these regions suggests that in both target availability conditions switch trials were associated with priority shifts, therefore supporting dynamic weighing of attentional relevance between target representation (see also van Driel et al., 2019).

5. Conclusion

We investigated the contributions of proactive and reactive control to target selection during multiple-target search. We found that both control mechanisms activate a similar network that has previously been associated with shifts of feature-based attention, with proactive control eliciting greater activity generally. In addition, proactive switching also activated other frontal regions that have been linked to free choice and evaluating alternative options other than the current action. We argue that these signals represent control processes to update target representations. The current study elucidates the behavioral and neural profiles of different target switching control strategies.

Conflicts of interest

The authors declare no conflict of interest.

Acknowledgements

This work was supported by Open Research Area Grant 464-13-003 from the Netherlands Organization for Scientific Research and by European Research Council Consolidator Grant ERC-2013-CoG-615423 to C. N. L. Olivers and by Open Research Area grant DFG PO 548/16-1 to S.Pollmann. We would like to thank Renate Blobel-Lüer and Jörg Stadler for technical and practical assistance during data collection and advice during data preprocessing, Michael Hanke and Falko Kaule for assistance during the setup phase of the study, and Tomas Knapen, Gilles de Hollander and especially Brónagh McCoy for valuable discussions about and suggestions for the fMRI analysis and drift diffusion modeling.

Appendix A. Supplementary data

Supplementary data to this article can be found online at https://doi.org/10.1016/j.neuroimage.2019.116133.

References

Abraham, A., Pedregosa, F., Eickenberg, M., Gervais, P., Muller, A., Kossaifi, J., Varoquaux, G., 2014. Machine learning for neuroimaging with scikit-learn. Front. Neuroinf. 8 (February), 1–10. http://doi.org/10.3389/fninf.2014.00014.

Arrington, C.M., Logan, G.D., 2004. The cost of a voluntary task switch. Psychol. Sci. 15 (9), 610–615. http://doi.org/10.1111/j.0956-7976.2004.00728.x.

Arrington, C.M., Logan, G.D., 2005. Voluntary task switching: chasing the elusive homunculus. J. Exp. Psychol. Learn. Mem. Cogn. 31 (4), 683–702. http://doi.org/10.1037/0278-7393.31.4.683.

Avants, B.B., Epstein, C.L., Grossman, M., Gee, J.C., 2008. Symmetric diffeomorphic image registration with cross-correlation: evaluating automated labeling of elderly and neurodegenerative brain. Med. Image Anal. 12 (1), 26–41. http://doi.org/10.1016/j.media.2007.06.004.

Badre, D., D'Esposito, M., 2009. Is the rostro-caudal axis of the frontal lobe hierarchical? Nat. Rev. Neurosci. 10 (9), 659–669. http://doi.org/10.1038/nrn2667.

Barrett, D.J.K., Zobay, O., 2014. Attentional control via parallel target-templates in dual-target search. PLoS One 9 (1), 1–9. http://doi.org/10.1371/journal.pone.0086848.

Behzadi, Y., Restom, K., Liau, J., Liu, T.T., 2007. A component based noise correction method (CompCor) for BOLD and perfusion based fMRI. Neuroimage 37 (1), 90–101. http://doi.org/10.1016/j.neuroimage.2007.04.042.

Botvinick, M., Nystrom, L.E., Fissell, K., Carter, C.S., Cohen, J.D., 1999. Conflict monitoring versus selection- for-action in anterior cingulate cortex. Nature 402 (11), 179–181. http://doi.org/10.1038/46035.

Brass, M., von Cramon, D.Y., 2004. Decomposing components of task preparation with functional magnetic resonance imaging. J. Cogn. Neurosci. 16 (4), 609–620. http://doi.org/10.1162/089892904323057335.

Braver, T.S., 2012. The variable nature of cognitive control: a dual mechanisms framework. Trends Cogn. Sci. 16 (2), 106–113. http://doi.org/10.1016/j.tics.2011.12.010.

Braver, T.S., Cohen, J.D., Nystrom, L.E., Jonides, J., Smith, E.E., Noll, D.C., 1997. A parametric study of prefrontal cortex involvement in human working memory. Neuroimage 5 (1), 49–62. http://doi.org/10.1006/nimg.1996.0247.

Braver, T.S., Paxton, J.L., Locke, H.S., Barch, D.M., 2009. Flexible neural mechanisms of cognitive control within human prefrontal cortex. Proc. Natl. Acad. Sci. U.S.A. 106 (18), 7351–7356. http://doi.org/10.1073/pnas.0808187106.

Braver, T.S., Reynolds, J.R., Donaldson, D.I., 2003. Neural mechanisms of transient and sustained cognitive control during task switching. Neuron 39 (4), 713–726. http://doi.org/10.1016/S0896-6273(03)00466-5.

Bunge, S.A., Kahn, I., Wallis, J.D., Miller, E.K., Wagner, A.D., 2003. Neural circuits subserving the retrieval and maintenance of abstract rules. J. Neurophysiol. 90 (5), 3419–3428. http://doi.org/10.1152/jn.00910.2002.

Bunge, S.A., Ochsner, K.N., Desmond, J.E., Glover, G.H., Gabrieli, J.D.E., 2001. Prefrontal regions involved in keeping information in and out of mind. Brain 124, 2074–2086. http://doi.org/10.1093/brain/124.10.2074.

Burgess, G.C., Braver, T.S., 2010. Neural mechanisms of interference control in working memory: effects of interference expectancy and fluid intelligence. PLoS One 5 (9), 1–11. http://doi.org/10.1371/journal.pone.0012861.

Cavanagh, J.F., Frank, M.J., 2014. Frontal theta as a mechanism for cognitive control. Trends Cogn. Sci. 18 (8), 414–421. http://doi.org/10.1016/j.tics.2014.04.012.

Cohen, M.X., 2014. A neural microcircuit for cognitive conflict detection and signaling. Trends Neurosci. 37 (9), 480–490. http://doi.org/10.1016/j.tins.2014.06.004.

Cole, M.W., Schneider, W., 2007. The cognitive control network: integrated cortical regions with dissociable functions. Neuroimage 37 (1), 343–360. http://doi.org/10.1016/j.neuroimage.2007.03.071.

Dale, A.M., Fischl, B., Sereno, M.I., 1999. Cortical surface-based analysis: I. Segmentation and surface reconstruction. Neuroimage 9 (2), 179–194. http://doi.org/10.1006/nimg.1998.0395.

Dalmaijer, E.S., Mathôt, S., Van der Stigchel, S., 2013. PyGaze: an open-source, cross-platform toolbox for minimal-effort programming of eyetracking experiments. Behav. Res. Methods 46, 913–921. http://doi.org/10.3758/s13428-013-0422-2.

de Hollander, G., Knapen, T., 2018. VU-Cog-Sci/nideconv: First Alpha Version Nideconv (Version v0.1.0). Zenodo. http://doi.org/10.5281/zenodo.1463839.

De Pisapia, N., Braver, T.S., 2006. A model of dual control mechanisms through anterior cingulate and prefrontal cortex interactions. Neurocomputing 69 (10–12), 1322–1326. http://doi.org/10.1016/j.neucom.2005.12.100.

Demanet, J., De Baene, W., Arrington, C.M., Brass, M., 2013. Biasing free choices: the role of the rostral cingulate zone in intentional control. Neuroimage 72, 207–213. http://doi.org/10.1016/j.neuroimage.2013.01.052.

Desimone, R., Duncan, J., 1995. Neural mechanisms of selective visual attention. Annu. Rev. Neurosci. 18 (1), 193–222. http://doi.org/10.1146/annurev.neuro.18.1.193.

Dombrowe, I., Donk, M., Olivers, C.N.L., 2011. The costs of switching attentional sets. Atten. Percept. Psychophys. 73, 2481–2488. http://doi.org/10.3758/s13414-011-0198-3.

Donner, T.H., Siegel, M., Fries, P., Engel, A.K., 2009. Buildup of choice-predictive activity in human motor cortex during perceptual decision making. Curr. Biol. 19 (18), 1581–1585. http://doi.org/10.1016/j.cub.2009.07.066.

Dosenbach, N.U.F., Fair, D.A., Cohen, A.L., Schlaggar, B.L., Petersen, S.E., 2008. A dual-networks architecture of top-down control. Trends Cogn. Sci. 12 (3), 99–105. http://doi.org/10.1016/j.tics.2008.01.001.

Dosenbach, N.U.F., Visscher, K.M., Palmer, E.D., Miezin, F.M., Wenger, K.K., Kang, H.C., Petersen, S.E., 2006. A core system for the implementation of task sets. Neuron 50 (5), 799–812. http://doi.org/10.1016/j.neuron.2006.04.031.

Dove, A., Pollmann, S., Schubert, T., Wiggins, C.J., Yves von Cramon, D., 2000. Prefrontal cortex activation in task switching: an event-related fMRI study. Cogn. Brain Res. 9 (1), 103–109. http://doi.org/10.1016/S0926-6410(99)00029-4.

Duncan, J., 2010. The multiple-demand (MD) system of the primate brain: mental programs for intelligent behaviour. Trends Cogn. Sci. 14 (4), 172–179. http://doi.org/10.1016/j.tics.2010.01.004.

Duprez, J., Gulbinaite, R., Cohen, M.X., 2018. Midfrontal theta phase coordinates behaviorally relevant brain computations during response conflict. BioRxiv 1–38. https://doi.org/10.1101/502716.

Elton, A., Gao, W., 2015. Task-positive functional connectivity of the default mode network transcends task domain. J. Cogn. Neurosci. 27 (12), 2369–2381. http://doi.org/10.1162/jocn.

Esteban, O., Markiewicz, C.J., Blair, R.W., Moodie, C.A., Isik, A.I., Erramuzpe, A., Gorgolewski, K.J., 2018. FMRIPrep: a robust preprocessing pipeline for functional MRI. Nat. Methods 1–10. http://doi.org/10.1038/s41592-018-0235-4.

Fedorenko, E., Duncan, J., Kanwisher, N., 2013. Broad domain generality in focal regions of frontal and parietal cortex. Proc. Natl. Acad. Sci. 110 (41), 16616–16621. http://doi.org/10.1073/pnas.1315235110.

Fonov, V., Evans, A., McKinstry, R., Almli, C., Collins, D., 2009. Unbiased nonlinear average age-appropriate brain templates from birth to adulthood. Neuroimage 47 (Suppl. 1), S102. http://doi.org/10.1016/S1053-8119(09)70884-5.

Forstmann, B.U., Brass, M., Koch, I., von Cramon, D.Y., 2006. Voluntary selection of task sets revealed by functional magnetic resonance imaging. J. Cogn. Neurosci. 18 (3), 388–398. http://doi.org/10.1162/jocn.2006.18.3.388.

Found, A., Müller, H.J., 1996. Searching for unknown feature targets on more than one dimension: investigating a "dimension-weighting" account. Percept. Psychophys. 58 (1), 88–101. http://doi.org/10.3758/BF03205479.

Gmeindl, L., Chiu, Y.C., Esterman, M.S., Greenberg, A.S., Courtney, S.M., Yantis, S., 2016. Tracking the will to attend: cortical activity indexes self-generated, voluntary shifts of attention. Atten. Percept. Psychophys. 78 (7), 2176–2184. http://doi.org/10.3758/s13414-016-1159-7.

Gorgolewski, K.J., Burns, C.D., Madison, C., Clark, D., Halchenko, Y.O., Waskom, M.L., Ghosh, S.S., 2011. Nipype: a flexible, lightweight and extensible neuroimaging data processing framework in Python. Front. Neuroinf. 5 (August). http://doi.org/10.3389/fninf.2011.00013.

Gorgolewski, K.J., Esteban, O., Markiewicz, C.J., Ziegler, E., Ellis, D.G., Jarecka, D., Ghosh, S., 2018. Nipy/Nipype: 1.1.6. http://doi.org/10.5281/ZENODO.1560596.

Gramfort, A., Luessi, M., Larson, E., Engemann, D.a., Strohmeier, D., Brodbeck, C., Hämäläinen, M., 2013. MEG and EEG data analysis with MNE-Python. Front. Neurosci. 7 (December), 1–13. http://doi.org/10.3389/fnins.2013.00267.

Greenberg, A.S., Esterman, M., Wilson, D., Serences, J.T., Yantis, S., 2010. Control of spatial and feature-based attention in frontoparietal cortex. J. Neurosci.: Off. J. Soc. Neurosci. 30 (43), 14330–14339. http://doi.org/10.1523/JNEUROSCI.4248-09.2010.

Greve, D.N., Fischl, B., 2009. Accurate and robust brain image alignment using boundary-based registration. Neuroimage 48 (1), 63–72. http://doi.org/10.1016/j.neuroimage.2009.06.060.

Hopfinger, J.B., Buonocore, M.H., Mangun, G.R., 2000. The neural mechanisms of top-down attentional control. Nat. Neurosci. 3 (3), 284–291. http://doi.org/10.1038/72999.

Huang, L., Pashler, H., 2007. A Boolean map theory of visual attention. Psychol. Rev. 114 (3), 599–631. http://doi.org/10.1037/0033-295X.114.3.599.

Huntenburg, J.M., 2014. Evaluating Nonlinear Coregistration of BOLD EPI and T1w Images. Doctoral Dissertation. Free University, Berlin.

Irlbacher, K., Kraft, A., Kehrer, S., Brandt, S.A., 2014. Mechanisms and neuronal networks involved in reactive and proactive cognitive control of interference in working memory. Neurosci. Biobehav. Rev. 46, 58–70. http://doi.org/10.1016/j.neubiorev.2014.06.014.

Ito, S., Stuphorn, V., Brown, J.W., Schall, J.D., 2003. Performance monitoring by the anterior cingulate cortex during saccade countermanding. Science 302 (5642), 120–122. http://doi.org/10.1126/science.1087847.

Jenkinson, M., Bannister, P., Brady, M., Smith, S.M., 2002. Improved optimization for the robust and accurate linear registration and motion correction of brain images. Neuroimage 17 (2), 825–841. http://doi.org/10.1016/S1053-8119(02)91132-8.

Jiang, J., Beck, J., Heller, K., Egner, T., 2015. An insula-frontostriatal network mediates flexible cognitive control by adaptively predicting changing control demands. Nat. Commun. 6 (May), 1–11. http://doi.org/10.1038/ncomms9165.

Jiang, J., Wagner, A.D., Egner, T., 2018. Integrated externally and internally generated task predictions Jointly guide cognitive control in prefrontal cortex. ELife 7, 1–23. http://doi.org/10.7554/eLife.39497.

Juola, J.F., Botella, J., Palacios, A., 2004. Task- and location-switching effects on visual attention. Percept. Psychophys. 66 (8), 1303–1317. http://doi.org/10.3758/BF03195000.

Karayanidis, F., Mansfield, E.L., Galloway, K.L., Smith, J.L., Provost, A., Heathcote, A., 2009. Anticipatory reconfiguration elicited by fully and partially informative cues that validly predict a switch in task. Cognit. Affect Behav. Neurosci. 9 (2), 202–215. http://doi.org/10.3758/CABN.9.2.202.

Kerns, J.G., Cohen, J.D., MacDonald, A.W., Cho, R.Y., Stenger, V.A., Carter, C.S., 2004. Anterior cingulate conflict monitoring and adjustments in control. Science 303 (5660), 1023–1026. http://doi.org/10.1126/science.1089910.

Kim, C., Cilles, S.E., Johnson, N.F., Gold, B.T., 2012. Domain general and domain preferential brain regions associated with different types of task switching: a meta-analysis. Hum. Brain Mapp. 33 (1), 130–142. http://doi.org/10.1002/hbm.21199.

Klein, A., Ghosh, S.S., Bao, F.S., Giard, J., Häme, Y., Stavsky, E., Keshavan, A., 2017. Mindboggling morphometry of human brains. PLoS Comput. Biol. 13 (2), e1005350. http://doi.org/10.1371/journal.pcbi.1005350.

Kloosterman, N.A., de Gee, J.W., Werkle-Bergner, M., Lindenberger, U., Garrett, D.D., Fahrenfort, J.J., 2019. Humans strategically shift decision bias by flexibly adjusting sensory evidence accumulation. ELife 8, e37321. https://doi.org/10.7554/eLife.3732.

Konishi, M., McLaren, D.G., Engen, H., Smallwood, J., 2015. Shaped by the past: the default mode network supports cognition that is independent of immediate perceptual input. PLoS One 10 (6), 1–18. http://doi.org/10.1371/journal.pone.0132209.

Liesefeld, H.R., 2018. Estimating the timing of cognitive operations with MEG/EEG latency measures: a primer, a brief tutorial, and an implementation of various methods. Front. Neurosci. 12 (October), 1–11. https://doi.org/10.3389/fnins.2018.00765.

Liston, C., Matalon, S., Hare, T.A., Davidson, M.C., Casey, B.J., 2006. Anterior cingulate and posterior parietal cortices are sensitive to dissociable forms of conflict in a task-switching paradigm. Neuron 50 (4), 643–653. http://doi.org/10.1016/j.neuron.2006.04.015.

Liu, T., Jigo, M., 2017. Limits in feature-based attention to multiple colors. Atten. Percept. Psychophys. 79, 2327–2337. http://doi.org/10.3758/s13414-017-1390-x.

Liu, T., Slotnick, S.D., Serences, J.T., Yantis, S., 2003. Cortical mechanisms of feature-based attentional control. Cerebr. Cortex 13 (12), 1334–1343. http://doi.org/10.1093/cercor/bhg080.

Luck, S.J., 2014. An Introduction to the Event-Related Potential Technique, second ed. MIT press, Cambridge, MA.

Maljkovic, V., Nakayama, K., 1994. Priming of pop-out: I. Role of features. Mem. Cogn. 22 (6), 657–672. http://doi.org/10.3758/BF03209251.

Mansouri, F.A., Koechlin, E., Rosa, M.G.P., Buckley, M.J., 2017. Managing competing goals — a key role for the frontopolar cortex. Nat. Neurosci. Rev. 18 (11), 645–657. http://doi.org/10.1038/nrn.2017.111.

Marklund, P., Persson, J., 2012. Context-dependent switching between proactive and reactive working memory control mechanisms in the right inferior frontal gyrus. Neuroimage 63 (3), 1552–1560. http://doi.org/10.1016/j.neuroimage.2012.08.016.

Mathôt, S., Schreij, D., Theeuwes, J., 2012. OpenSesame: an open-source, graphical experiment builder for the social sciences. Behav. Res. Methods 44 (2), 314–324. http://doi.org/10.3758/s13428-011-0168-7.

Meiran, N., 1996. Reconfiguration of processing mode prior to task performance. J. Exp. Psychol. Learn. Mem. Cogn. 22 (6), 1423–1442. http://doi.org/10.1037/0278-7393.22.6.1423.

Meiran, N., 2010. Task switching and cognitive self control. In: Self Control in Society, Mind and Brain, pp. 202–220. http://doi.org/10.1093/acprof:oso/9780195391381.001.0001.

Menneer, T., Barrett, D.J.K., Phillips, L., Donnelly, N., Cave, K.R., 2007. Costs in searching for two targets: dividing search across target types could improve airport security screening. Appl. Cognit. Psychol. 21, 915–932. http://doi.org/10.1002/acp.1305.

Menon, V., Uddin, L.Q., 2010. Saliency, switching, attention and control: a network model of insula function. Brain Struct. Funct. 214 (5–6), 655–667. http://doi.org/10.1007/s00429-010-0262-0.

Miller, E.K., Cohen, J.D., 2001. An integrative theory of prefrontal cortex function. Annu. Rev. Neurosci. 24, 167–202. https://doi.org/10.1146/annurev.neuro.24.1.167.

Miller, J., Patterson, T., Ulrich, R., 1998. Jackknife-based method for measuring LRP onset latency differences. Psychophysiology 35 (1), 99–115. https://doi.org/10.1111/1469-8986.3510099.

Moore, K.S., Weissman, D.H., 2010. Involuntary transfer of a top-down attentional set into the focus of attention: evidence from a contingent attentional capture paradigm. Atten. Percept. Psychophys. 72 (6), 1495–1509. https://doi.org/10.3758/APP.72.6.1495.

Morey, R.D., 2008. Confidence intervals from normalized data: a correction to cousineau (2005). Tutorials. Quant. Methods. Psychol. 4 (2), 61–64. http://doi.org/10.3758/s13414-012-0291-2.

Niendam, T.A., Laird, A.R., Ray, K.L., Dean, Y.M., Glahn, D.C., Carter, C.S., 2012. Meta-analytic evidence for a superordinate cognitive control network subserving diverse executive functions. Cognit. Affect Behav. Neurosci. 12 (2), 241–268. http://doi.org/10.3758/s13415-011-0083-5.

Oberauer, K., 2002. Access to information in working memory: exploring the focus of attention. J. Exp. Psychol. Learn. Mem. Cogn. 28 (3), 411–421. http://doi.org/10.1037/0278-7393.28.3.411.

Olivers, C.N.L., Eimer, M., 2011. On the difference between working memory and attentional set. Neuropsychologia 49 (6), 1553–1558. http://doi.org/10.1016/j.neuropsychologia.2010.11.033.

Olivers, C.N.L., Peters, J., Houtkamp, R., Roelfsema, P.R., 2011. Different states in visual working memory: when it guides attention and when it does not. Trends Cogn. Sci. 15 (7), 327–334. http://doi.org/10.1016/j.tics.2011.05.004.

Orr, J.M., Banich, M.T., 2013. The neural mechanisms underlying internally and externally guided task selection. Neuroimage 80309 (303), 1–30. http://doi.org/10.1016/j.neuroimage.2013.08.047.

Ort, E., Fahrenfort, J.J., Olivers, C.N.L., 2017. Lack of free choice reveals the cost of having to look for more than one object. Psychol. Sci. 28 (8), 1137–1147. http://doi.org/10.1177/0956797617705667.

Ort, E., Fahrenfort, J.J., Olivers, C.N.L., 2018. Lack of free choice reveals the cost of multiple-target search within and across feature dimensions. Atten. Percept. Psychophys. (80), 1904–1917. http://doi.org/10.3758/s13414-018-1579-7.

Ort, E., Fahrenfort, J.J., ten Cate, T., Olivers, C.N.L., 2019. Humans can efficiently look for, but not select multiple visual objects. bioRxiv. http://doi.org/10.1101/653030v1.

Passingham, R.E., Bengtsson, S.L., Lau, H.C., 2010. Medial frontal cortex: from self-generated action to reflection on one's own performance. Trends Cogn. Sci. 14 (1), 16–21. http://doi.org/10.1016/j.tics.2009.11.001.

Poldrack, R.A., Mumford, J.A., Nichols, T.E., 2011. Handbook of Functional MRI Data Analysis. Cambridge University Press, Cambridge. https://doi.org/10.1017/CBO9780511895029.

Pollmann, S., 2016. Frontopolar resource allocation in human and nonhuman primates. Trends Cogn. Sci. 20 (2), 84–86. http://doi.org/10.1016/j.tics.2015.11.006.

Pollmann, S., Weidner, R., Müller, H.J., Maertens, M., von Cramon, D.Y., 2006. Selective and interactive neural correlates of visual dimension changes and response changes. Neuroimage 30 (1), 254–265. http://doi.org/10.1016/j.neuroimage.2005.09.013.

Pollmann, S., Weidner, R., Müller, H.J., von Cramon, D.Y., 2000. A fronto-posterior network involved in visual dimension changes. J. Cogn. Neurosci. 12 (3), 480–494. http://doi.org/10.1162/089892900562156.

Power, J.D., Mitra, A., Laumann, T.O., Snyder, A.Z., Schlaggar, B.L., Petersen, S.E., 2014. Methods to detect, characterize, and remove motion artifact in resting state fMRI. Neuroimage 84, 320–341. http://doi.org/10.1016/j.neuroimage.2013.08.048.

Power, J.D., Petersen, S.E., 2013. Control-related systems in the human brain. Curr. Opin. Neurobiol. 23 (2), 223–228. http://doi.org/10.1016/j.conb.2012.12.009.

Raichle, M.E., 2015. The brain's default mode network. Annu. Rev. Neurosci. 38 (1), 433–447. http://doi.org/10.1146/annurev-neuro-071013-014030.

Raichle, M.E., Macleod, A.M., Snyder, A.Z., Powers, W.J., Gusnard, D.A., Shulman, G.L., 2001. A default mode of brain function. Proc. Natl. Acad. Sci. 98 (2), 676–682. http://doi.org/10.1073/pnas.98.2.676.

Ratcliff, R., Rouder, J.N., 1998. Modeling response times for two-choice decisions. Psychol. Sci. 9 (5), 347–356. http://doi.org/10.1111/1467-9280.00067.

Ryman, S.G., El Shaikh, A.A., Shaff, N.A., Hanlon, F.M., Dodd, A.B., Wertz, C.J., Mayer, A.R., 2018. Proactive and reactive cognitive control rely on flexible use of the ventrolateral prefrontal cortex. Hum. Brain Mapp. (January), 1–12. http://doi.org/10.1002/hbm.24424.

Rypma, B., D'Esposito, M., 1999. The roles of prefrontal brain regions in components of working memory: effects of memory load and individual differences. Proc. Natl. Acad. Sci. 96 (11), 6558–6563. http://doi.org/10.1073/pnas.96.11.6558.

Schmitz, F., Voss, A., 2012. Decomposing task-switching costs with the diffusion model. J. Exp. Psychol. Hum. Percept. Perform. 38 (1), 222–250. http://doi.org/10.1037/a0026003.

Seeley, W.W., Menon, V., Schatzberg, A.F., Keller, J., Glover, G.H., Kenna, H., Greicius, M.D., 2007. Dissociable intrinsic connectivity networks for salience processing and executive control. J. Neurosci. 27 (9), 2349–2356. http://doi.org/10.1523/JNEUROSCI.5587-06.2007.

Shenhav, A., Botvinick, M.M., Cohen, J.D., 2013. The expected value of control: an integrative theory of anterior cingulate cortex function. Neuron 79 (2), 217–240. http://doi.org/10.1016/j.neuron.2013.07.007.

Shulman, G.L., 2002. Two attentional processes in the parietal lobe. Cerebr. Cortex 12 (11), 1124–1131. http://doi.org/10.1093/cercor/12.11.1124.

Singmann, H., Bolker, B., Westfall, J., Aust, F., Højsgaard, S., Fox, J., Love, J., 2016. Afex: Analysis of Factorial Experiments. R Package Version 0.16-1. R Package Version 0.16-1.

Slagter, H.A., Giesbrecht, B., Kok, A., Weissman, D.H., Kenemans, J.L., Woldorff, M.G., Mangun, G.R., 2007. fMRI evidence for both generalized and specialized components of attentional control. Brain Res. 1177 (1), 90–102. http://doi.org/10.1016/j.brainres.2007.07.097.

Slagter, H.A., Weissman, D.H., Giesbrecht, B., Kenemans, J.L., Mangun, G.R., Kok, A., Woldorff, M.G., 2006. Brain regions activated by endogenous preparatory set shifting as revealed by fMRI. Cognit. Affect Behav. Neurosci. 6 (3), 175–189. http://doi.org/10.3758/CABN.6.3.175.

Smallwood, J., Tipper, C., Brown, K., Baird, B., Engen, H., Michaels, J.R., Schooler, J.W., 2013. Escaping the here and now: evidence for a role of the default mode network in perceptually decoupled thought. Neuroimage 69, 120–125. http://doi.org/10.1016/j.neuroimage.2012.12.012.

Smith, A.B., Taylor, E., Brammer, M., Rubia, K., 2004. Neural correlates of switching set as measured in fast, event-related functional magnetic resonance imaging. Hum. Brain Mapp. 21 (4), 247–256. http://doi.org/10.1002/hbm.20007.

Smith, S.M., Brady, J.M., 1997. Susan - a new approach to low level image processing. Int. J. Comput. Vis. 23 (1), 45–78. http://doi.org/10.1023/A:1007963824710.

Smith, S.M., Nichols, T.E., 2009. Threshold-free cluster enhancement: addressing problems of smoothing, threshold dependence and localisation in cluster inference. Neuroimage 44 (1), 83–98. http://doi.org/10.1016/j.neuroimage.2008.03.061.

Smith, V., Mitchell, D.J., Duncan, J., 2018. Role of the default mode network in cognitive transitions. Cerebr. Cortex 28 (October), 3685–3696. http://doi.org/10.1093/cercor/bhy167.

Sohn, M.-H., Ursu, S., Anderson, J.R., Stenger, V.A., Carter, C.S., 2000. The role of prefrontal cortex and posterior parietal cortex in task switching. Proc. Natl. Acad. Sci. 97 (24), 13448–13453. https://doi.org/10.1073/pnas.240460497.

Soon, C.S., Brass, M., Heinze, H.J., Haynes, J.D., 2008. Unconscious determinants of free decisions in the human brain. Nat. Neurosci. 11 (5), 543–545. http://doi.org/10.1038/nn.2112.

Spitzer, B., Haegens, S., 2017. Beyond the status quo: a role for beta oscillations in endogenous content (Re-) activation. Eneuro 4 (4). http://doi.org/10.1523/ENEURO.0170-17.2017.

Spreng, R.N., 2012. The fallacy of a "task-negative" network. Front. Psychol. 3 (MAY), 1–5. http://doi.org/10.3389/fpsyg.2012.00145.

Spreng, R.N., DuPre, E., Selarka, D., Garcia, J., Gojkovic, S., Mildner, J., Turner, G.R., 2014. Goal-congruent default network activity facilitates cognitive control. J. Neurosci. 34 (42), 14108–14114. http://doi.org/10.1523/JNEUROSCI.2815-14.2014.

Taylor, P.C.J., Rushworth, M.F.S., Nobre, A.C., 2008. Choosing where to attend and the medial frontal cortex: an FMRI study. J. Neurophysiol. 100 (3), 1397–1406. https://doi.org/10.1152/jn.90241.2008.

Treiber, J.M., White, N.S., Steed, T.C., Bartsch, H., Holland, D., Farid, N., Chen, C.C., 2016. Characterization and correction of geometric distortions in 814 diffusion weighted images. PLoS One 11 (3), e0152472. http://doi.org/10.1371/journal.pone.0152472.

Tustison, N., Avants, B.B., Cook, P.A., Zheng, Y., Egan, A., Yushkevich, P.U., Gee, J.C., 2010. N4ITK: improved N3 bias correction. IEEE Trans. Med. Imaging 29.

Ullsperger, M., Danielmeier, C., Jocham, G., 2014. Neurophysiology of performance monitoring and adaptive behavior. Physiol. Rev. 94 (1), 35–79. http://doi.org/10.1152/physrev.00041.2012.

van Driel, J., Ort, E., Fahrenfort, J.J., Olivers, C.N.L., 2019. Beta and theta oscillations differentially support free versus forced control over multiple-target search. J. Neurosci. 149, 114–128. https://doi.org/10.1523/JNEUROSCI.2547-18.2018.

Vatansever, D., Menon, D.K., Stamatakis, E.A., 2017. Default mode contributions to automated information processing. Proc. Natl. Acad. Sci. 114 (48), 12821–12826. http://doi.org/10.1073/pnas.1710521114.

Wager, T.D., Jonides, J., Reading, S., 2004. Neuroimaging studies of shifting attention: a meta-analysis. Neuroimage 22 (4), 1679–1693. http://doi.org/10.1016/j.neuroimage.2004.03.052.

Wang, S., Peterson, D.J., Gatenby, J.C., Li, W., Grabowski, T.J., Madhyastha, T.M., 2017. Evaluation of field map and nonlinear registration methods for correction of susceptibility artifacts in diffusion MRI. Front. Neuroinf. 11, 17. http://doi.org/10.3389/fninf.2017.00017.

Wiecki, T.V., Sofer, I., Frank, M.J., 2013. HDDM: hierarchical bayesian estimation of the drift-diffusion model in Python. Front. Neuroinf. 7 (August), 1–10. http://doi.org/10.3389/fninf.2013.00014.

Winkler, A.M., Ridgway, G.R., Webster, M.A., Smith, S.M., Nichols, T.E., 2014. Permutation inference for the general linear model. Neuroimage 92, 381–397. http://doi.org/10.1016/j.neuroimage.2014.01.060.

Wisniewski, D., Goschke, T., Haynes, J.D., 2016. Similar coding of freely chosen and externally cued intentions in a fronto-parietal network. Neuroimage 134, 450–458. http://doi.org/10.1016/j.neuroimage.2016.04.044.

Wisniewski, D., Reverberi, C., Tusche, A., Haynes, J.D., 2015. The neural representation of voluntary task-set selection in dynamic environments. Cerebr. Cortex 25 (12), 4715–4726. http://doi.org/10.1093/cercor/bhu155.

Woolrich, M.W., Ripley, B.D., Brady, M., Smith, S.M., 2001. Temporal autocorrelation in univariate linear modeling of FMRI data. Neuroimage 14 (6), 1370–1386. http://doi.org/10.1006/nimg.2001.0931.

Wu, J., Ngo, G.H., Greve, D., Li, J., He, T., Fischl, B., Yeo, B.T.T., 2018. Accurate nonlinear mapping between MNI volumetric and FreeSurfer surface coordinate systems. Hum. Brain Mapp. 39 (9), 3793–3808. http://doi.org/10.1002/hbm.24213.

Zhang, J., Kriegeskorte, N., Carlin, J.D., Rowe, J.B., 2013. Choosing the rules: distinct and overlapping frontoparietal representations of task rules for perceptual decisions. J. Neurosci. 33 (29), 11852–11862. http://doi.org/10.1523/JNEUROSCI.5193-12.2013.

Zhang, Y., Brady, M., Smith, S.M., 2001. Segmentation of brain MR images through a hidden Markov random field model and the expectation-maximization algorithm. IEEE Trans. Med. Imaging 20 (1), 45–57. http://doi.org/10.1109/42.906424.